The Influence of nC$_{60}$ on Hydroxyl Radicals (·OH)

A study to determine the accountability of C$_{60}$ aggregates on the photochemical production of hydroxyl radicals (·OH) in various solutions, and the influence of other water quality parameters.

A Major Qualifying Project submitted to the faculty of
Worcester Polytechnic Institute in partial fulfillment of the requirements
for the Degree of Bachelor of Science in Civil Engineering, Environmental
Focus

SUBMITTED TO:
  On-Site Liaison: Professor Zhang Bo Shanghai Jiao Tong University
  Project Advisor: Professor John Bergendahl Worcester Polytechnic Institute
  Project Co-advisors: Professor David DiBiasio Worcester Polytechnic Institute
                      Professor Nathaniel Deskins Worcester Polytechnic Institute

SUBMITTED BY:

Kelsey Lea Snyder
April 28, 2016

Abstract

Nano-materials have become widespread in various applications and research topics, finding its way into the aquatic environment. Thus causing concern regarding its potential toxicity to humans. This particular study looks specifically at stable colloidal nano-C_{60}(nC_{60}) aggregates and its capability to produce or quench hydroxyl radicals ($\cdot OH$) by altering pH, concentration and reaction time. Terephlatic acid (TA) was the main component in witnessing the production of these radicals and how nC_{60} affected each solution. With decrease in concentration of TA there was a corresponding decrease in OH production. Analysis also showed the outside media having a lower pH value proved to quench the production as well. Ultraviolet-A irradiation or constant stirring for a longer reaction time eventually led to $\cdot OH$ production; dependent on their exact composition. Multiple works support that nC_{60} aggregates and its physiochemical properties associated with toxicity are dependent on the surrounding environment and its conditions.

Acknowledgements

Thank you to advisor Professor Bergendahl of Worcester Polytechnic Institute for all your encouragement and support through this journey. To co- advisors Professor DiBiasio and Professor Deskins a special thank you. As well as a thank you to Professor Zhang Bo of Shanghai Jiao Tong University for allowing this project to be researched in the Shanghai Jiao Tong Minhang Campus Water Pollution Control Laboratory. Additional thanks are owed to Shanghai Jiao Tong University Research Assistant and PhD candidate Ge Ling for the guidance and help provided throughout my term abroad.

Table of Contents

Table of Figures

Table of Tables

Executive Summary

Harold W. Kroto, Robert F. Curl and Richard E. Smalley noted the first discovery of fullerenes at Rice University in 1985. Observing the spherical shape and correlating it to that of a geodesic dome, created by architect Richard Buckminster Fuller, allowed for the perfect name of buckminsterfullerene. Buckminsterfullerene's or "buckyballs", have several resonance structures illustrated later in the study varying from spherical, elliptical and tubular form. C_{60} is created of exclusively 60 carbon atoms, 60 vertices and 32 faces. Having both single and double bonds at its vertices allowing all its valences to be satisfied. C_{60} having a cage like structure, small size, insolubility and high reactivity give an extremely wide range for existing applications.

The rapid increase involving C_{60} also increases the inevitable release into the environment. Due to being practically insoluble as C_{60}, it makes its way through the environment and ultimately ends its journey in various aquatic conditions forming nano-C_{60} (nC_{60}) aggregates ranging from 5 – 500 nanometers (nm). Formulating these aggregates altered than the original properties pertaining to pure C_{60}. Therefore n C_{60} specifically had become a crucial topic for observation and discussion. It has been discovered that nC_{60} have photochemical properties that lead to the production of varying reactive oxygen species (ROS), each altering the effects on any given biological system.

ROS have been distinguished as being one of the large contributors in toxicity related studies and its potentially harmful effects on humans. Reactive oxygen species are linked to many methods of formulation, ionizing radiation, lipid peroxidation or oxidative stress. Those were only a few possibilities each with supporting material concerning back to the toxicity caused by that individual formation of ROS.

With multiple ways for creation left multiple ways to observe the ROS production. In this study Ultraviolet-A irradiation and magnetic stirrers were used to promote one form of ROS, a hydroxyl radical ($\cdot$OH) specifically. Terephlatic acid (TA) and 4-chlorobenzoic acid (pCBA) were used as a synthetic biological systems in these distinct trials. Both being an $\cdot$OH scavenger which is produced given the H_2O_2 upon UV, allowed for fluorescence emission and the degradation rates to be observed.

Using spectrophotometry to measure the fluorescence spectra of each solution following the different reaction times illustrated the diverse effects to each solution and how they were associated with nC_{60} in each given trial. The High Performance Liquid Chromatography (HPLC) machine recorded the retention time, area under peak and height of the peak. The degradation rate pertained to pCBA and was in direct correlation to the production of the $\cdot$OH in the 6 trials using HPLC.

Altering pH, concentration, ionic strength and reaction are but some alterations that clarified as being vital in determining the physiochemical and photochemical properties of nC_{60}. Consequently it has been noted to change the transport behavior of n nC_{60} completely and its potential risks for toxicity amongst humans.

Previous research by Shanhai Jiao Tong University (SJTU) in the exploration of nC_{60} aggregates and its affects on different aqueous parameters proved it had the capability for photochemical reactivity. It also depicted that environmental influences on a given system have significant influence on nC_{60} and its properties. Studies have shown differences as well as similarities between them, however, not one can definitively state that toxicity is strictly based on the involvement of nC_{60} in a given biological system. The studies only confirm that the toxicity is relative to the influence by nC_{60} and its physiochemical properties as well as the alterations to the media surrounding nC_{60}.

Design Statement

This project fulfills the requirements for the Major Qualifying Project (MQP) in the Civil Engineering Department at Worcester Polytechnic Institute by incorporating a fundamental design portion.

The goal of this project was to formulate nano-C_{60} (nC_{60}) aggregates and test for the production of hydroxyl radicals in varying aqueous solutions. This study examined how altering the physiochemical properties of nC_{60} affected a given solution. The outside media was monitored and carefully adjusted to comprehend which characteristics had any inverse effect on nC_{60}.

First, background knowledge of nC_{60} and hydroxyl radicals was gathered. Secondly, several trial studies were devised and executed to better observe each effect associated with foreign matter. Experiments were intended to correlate whether the toxicity present was a resultant of nC_{60}. Data found allowed for the design of a full-scale reactor in an operational treatment system and its feasibility. Lastly, recommendations and future research opportunities were postulated considering the growing demand for nC_{60} and other carbon allotropes.

Professional Licensure

The National Council of Examiners for Engineering and Surveying (NCEES) provides individuals with the ability to obtain the highest level of accomplishments and respect in the field of engineering with the professional engineering licensure (PE). The PE license is a symbol of respect and honor among colleagues and clients. Licensed engineers have the ability to sign and seal engineering drawings and plans to public authorities for approval. Individuals that are a PE must hold themselves to a higher professional and ethical standard than other engineers in the field.

In order to achieve the prestige of being a PE, a series of specific requirements must be completed: earn an engineering degree from a four year accredited engineering program, successfully complete the Fundamentals of Engineering (FE) exam, achieve four years of engineering experience alongside an experienced PE and complete the Principles and Practice of Engineering (PE) exam. Once the exam is passed, the life of a dedicated professional engineer is far from over. Continuing educational courses and various professional opportunities are required to maintain the PE license.

The PE is more than just a prestige award; it develops one's career by demonstrating commitment and leadership to the engineering profession. The PE brings the responsibility and importance of maintaining a professional and ethical persona at home and in the work place.

The importance of the licensure is far greater than an individual award; it is a symbol of respect and comfort to the public. The decisions and actions that a PE makes may directly or indirectly alter the lives of not only the individual but also the public around them. With the ability that an engineer has to greatly affect the lives of people around them, the licensure provides a professional standard for all engineers to aspire towards.

Introduction

A fullerene was discovered in 1985 by researchers from Rice University. It is any molecule composed entirely of carbon atoms. There are different forms associated with fullerenes including a hollow sphere, ellipsoid or a tube. Each form of fullerene has the potential to expand both positively and negatively in the world.

Fullerenes were named for their association with Richard Buckminster Fuller. He was an architectural modeler, made famous for the creation of the geodesic dome. The similar shape of spherical fullerenes to the geodesic dome allowed for a perfectly relevant nickname. Spherical fullerenes are commonly known as "buckyballs," while the cylindrical forms are referred to as "nanotubes" or "buckytubes".

The fullerene C_{60} is the main foundation for the following study. C_{60} is virtually insoluble; however, it has the ability to form water-stable aggregates of various diameters. nC_{60} is nano-scale aggregates derived from C_{60} molecules with a diameter ranging from a size of 5-500 nm in diameter. (G.V. Andrievsky, V.K. Klochkov, E.L. Karyakina, N.O. Mchedlov-Petrossyan 1999).

In performing several types of experiments to further investigate nC_{60} we might be able to determine whether these aggregates promote or quench the photochemical production of hydroxyl radicals ($\cdot OH$) in different solutions Altering different elements in each solution in turn caused noticeable differences to the corresponding results.

Hydroxyl radicals or $\cdot OH$ radicals cannot be measured directly during an ozonation process, thus the probes provided in the following experiments, terephlatic acid (TA) and 4-chlorobenzic acid (pCBA). These probes are known $\cdot OH$ scavengers, being used it allowed to better witness the production or quenching of the hydroxyl radicals. Using UV-A irradiation and magnetic stir plates as the promoting factor of $\cdot OH$.

Spectrophotometry is the quantitative measurement of the reflection or transmission properties of a material as a function of λ, representing wavelength (nm). This measurement of fluorescence spectra was the main focus in this study with brief analysis in High Performance Liquid Chromatography.

The results obtained from this study proved the quenching of hydroxyl radicals to be just as real as the production of them. The greater the time spent in the UV-reactor or on a magnetic stir place, the greater the production of hydroxyl radicals ($\cdot$OH). The graphs proved with longer reaction time showed a greater increase of fluorescence correlating directly with the production of $\cdot$OH.

When the concentration of TA was increased, the ability to produce $\cdot$OH increased as well as its fluorescence spectra. The pH largely affected the size of the aggregates in the solution, in turn changing the surface area of the aggregates and its surface charge. The lower the pH in a given solution showed hardly any production of $\cdot$OH, whereas a higher pH of the surrounding media caused a spike in fluorescence.

There was a large amount of variable change in this study that allowed for the testing to be flexible. For further research into nC_{60} and its effects on hydroxyl radicals, production should be taken more in depth with more consistent controls and a vast array of different media solutions. With furthering research it will aid in the determination if nC_{60} is in fact the cause of toxicity among different biological systems and what alterations can be made to generate the desired result.

Background

Fullerenes

Fullerenes were discovered in 1985 by researchers at Rice University. In 1996 Harold W. Kroto, Robert F. Curl and Richard E. Smalley won the Nobel Prize for Chemistry due to their discovery of fullerenes. Fullerenes are molecules composed entirely of carbon. There are different forms associated with fullerenes including a hollow sphere, ellipsoid and a tube. Each form of fullerene has the potential for further research that will advance the chemical and technical aspects of each material.

Fullerenes were named for their association with Richard Buckminster Fuller. He was an architectural modeler, made famous for the creation of the geodesic dome. The similar shape of spherical fullerenes to the geodesic dome allowed for a perfectly relevant nickname. Spherical fullerenes are commonly known as "buckyballs," while the cylindrical forms are referred to as "nanotubes" or "buckytubes". **Figure 1** depicts several forms of carbon and its allotropes.
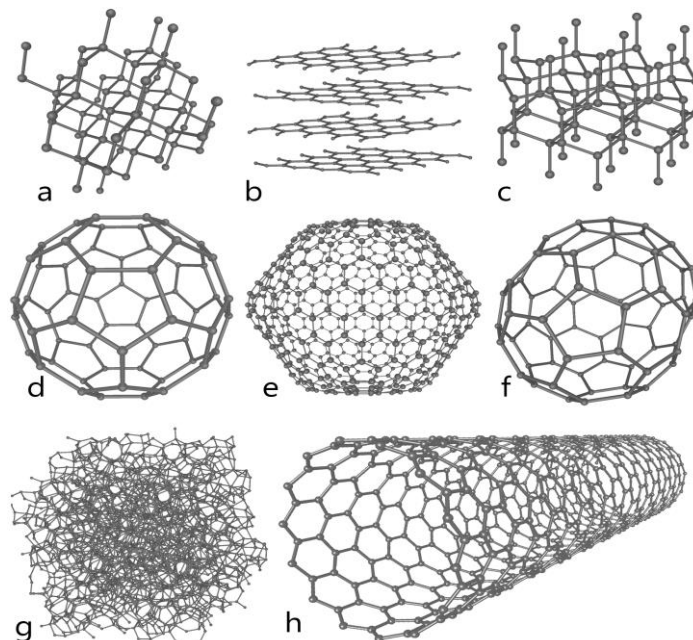
Figure 1: Multiple Various Carbon Allotropes (i.e. diamond, graphite, lonsdaleite, fullerene C_{60}, fullerene C_{540}, fullerene C_{70}, amorphous carbon and carbon nanotube respectively) (Boundless 2015)

Previously only limited amounts of fullerenes could be generated naturally; as the demand for fullerene testing rapidly increased, there have been advancements in the techniques to develop larger quantities more efficiently. The earliest method for fullerene production called for an inert atmosphere allowing for laser vaporization of carbon molecules. Production of fullerenes for prospective investigations had been noted to be in a chaotic electric-arc process undergoing temperatures exceeding 3000 K (Ventra, Evoy and Heflin 2004).

C_{60}

This fullerene is the main foundation for the following study and a strong example of a spherical form. Buckyballs have many resonance structures; in this particular case C_{60} is composed of 60 carbon atoms, 60 vertices and 32 faces. A C_{60} molecule has 12 faces, which are pentagonal shaped; the remaining 20 faces are hexagonal. At each of the vertices of this molecule there is a carbon atom with two single bonds and one double bond, allowing all valences to be satisfied.

In 1990 a new instrument was created to produce larger quantities of C_{60} from an electric-arc apparatus. This process demands Helium gas to be pumped down and released into the chamber; this is then repeated. The bell jar is then filled with roughly 100 Torr of Helium. It is all connected to a power supply in the welding kit and is turned on for 10-15 seconds. This step results in a large amount of black soot produced in the bell jar. After roughly 5-10 minutes of a cool down period the bell jar equalizes with atmospheric pressure. The bell jar is removed from the apparatus and the glass surfaces are scraped to collect the material. Of the collected material 10% of the soot is made up of C60 and extracted from the soot using a small amount of toluene. Figure 2 provides an image for the Kratschmer-Huffman apparatus and the different mechanisms undergone to achieve the production of fullerenes.
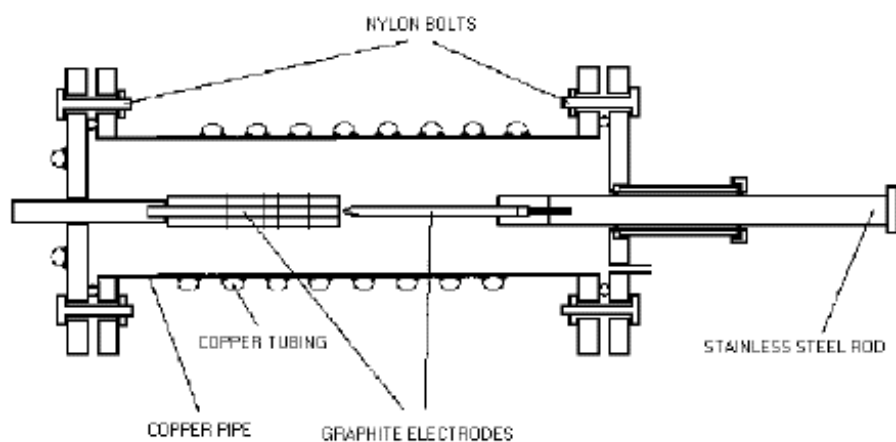
Figure 2: Kratschmer-Huffman Apparatus (Unwin 1990)

Pure C_{60} was thought to be hydrophobic since it is nonpolar and symmetrical (Jung, Wang and Jang 2009). Obtaining pure C_{60} is achieved through liquid chromatography. The combination of chemicals is dissolved in toluene and pumped through a column of activated charcoal, followed by a mixing with silica gel. C_{60} appears as a magenta color at first, followed by C_{70}, which appears red in color. Both solutions are collected separately and toluene is used as the extraction solvent and is later removed by a rotary evaporator.

It was acknowledged during these studies that the product (mainly C_{60} and C_{70}) is soluble in various non-polar solvents including toluene, benzene and carbon disulfide (Ventra, Evoy and Heflin 2004). C_{60} is virtually insoluble; however, it has the ability to form water-stable aggregates of various diameters.

Nano-C$_{60}$ aggregates

As research and technology thrive the demand for nano-materials is rapidly increasing. Throughout the different industries extensive studies and vast consumer products being tested for fabrication pose an amplified risk of fullerenes being released into the environment. Research verified C$_{60}$ could be solubilized a few ways, by solvent extraction or the vigorous stirring of C$_{60}$ in water (Ventra, Evoy and Heflin 2004). The colloidal aggregates diameter vary anywhere a size of 5-500 nm in diameter. (Andrievsky, et al. 1999).

Unintentionally, nC$_{60}$ molecules made the journey into the environment and it was observed that after a certain point, human contact indirectly or directly was unavoidable (Andrievsky, et al. 1999). Vast categories of research pertaining to nC$_{60}$ aggregates have in turn lead to a vast array of data collected. Scientists noted that there are many different physicochemical parameters related to the aggregation state of a fullerene and their derivatives. Each parameter could play a small or large role in determining its bioavailability as well as reactivity (Andrievsky, et al. 1999). Thus, making it essential to find out as much general data on nC$_{60}$ as possible and the potential affects it could have on a biological system.

Biological Systems

A biological system is comprised of a complex network of related entities such as cells, tissues, organs etc. to work toward a common function. In these types of systems not one thing can function independently proving their intricacy and viability. It is not always directly in relation to a human and its systems such as the respiratory system, digestive system or even nervous system.

Today's modern classification of systems depicts a more in depth and having multiple levels of hierarchical organization. Darwin's theory of evolution plays a large role in these classifications. A taxonomic system links structural and physiological traits between organisms. A simpler way to associate taxonomy is looking at the Greek origin of 'taxis-nomia' meaning 'arrangement distribution'. Naming them and arranging them, to properly name and categorize them in a way that makes sense scientifically.

The other being a phylogenic classification, were it is based solely on genetic connections. Phylogenetic is the field within biology that reconstructs evolutionary history and studies the patterns of relationships among organisms. Science is like history in the case of experimental research given no experiment will be flawlessly exact. There will be variable changes throughout and one can only use history and current data to try and duplicate desired results or alter them at hopes to achieve them. Phylogenic systems are present in the following study of nC_{60}.

Natural Organic Matter

Natural organic matter (NOM) is the material present in ground or surface water. NOM is collected from any living or growing organism, humic and non-humic. A generalized rule of thumb is that most organic material contains carbon. Once the organism(s) dies, the matter decomposes and the organic matter is broken down and becomes NOM ranging from 200-20,000 amu (DiToro 2012). NOM is generally classified by solubility, as measured by particle size. Colloidal or particulates are roughly 0.45 micron or greater, while those below 0.45 micron are categorized as dissolved.

Ultrafiltration membranes are one of the most standard methods for removal of various NOM. Using hydrostatic pressures to force water and other liquids through the semipermeable membrane, the pores are meant to trap every particle. The pore size of the ultrafiltration membrane ranges from 0.1-0.001 microns. NOM, smaller in size than the pore cannot be fully removed with conventional water treatment practices. Some NOM have shown the ability to produce by-products such as trihalomethane during disinfection. Raw water from surfaces and/or ground water sources show the dissolved fraction is the major source for NOM, risking the production of by-products.

DiToro's study was to test ultrafiltration membranes in original form and some that have been manually altered to a negative charge. A UV800 Spectrophotometer was used to test five solutions and one of distilled water as control pre and post filtration. The absorbance and concentration from pre-filtration was recorded and plotted, a standard curve line for humic-based NOM was obtained. Post filtration was compared to the original absorption levels to calculate the remaining concentration of NOM. "It was determined that a negative charge modification of the membrane was an appropriate method to remove NOM and reduce membrane fouling, due to the electrostatic interaction between the charged membrane and the particulate compounds in the water, and with the membrane pore size" (DiToro 2012).

Inorganic Matter

Generally inorganic matter is derived from things such as minerals, metals, and rocks none of which contain carbon. It mainly contains oxides and sulfides that are firmly inorganic. While there are always exceptions to a rule there are various inorganic compounds that do in fact contain carbon, carbon monoxide, carbon dioxide, carbides, thiocyanates, etc.

Inorganic materials come from many sources and can be found in many formats. A paper-based format of inorganic material could include photos containing metallic particles, ink of different pigments derived from different minerals. As well as many inorganic materials can be found in the world naturally but can also be manufactured in society to generate more or new forms of materials.

Reactive Oxygen Species

The generation of reactive oxygen species (ROS) is a natural consequence of aerobic metabolism (Di Giulio and Meyer 2008). ROS are chemically reactive molecules that have formed as a natural byproduct of the normal breakdown of oxygen. Free radicals, superoxide anion ($O^{\bullet}_2{}^-$), hydroxyl radicals ($^{\bullet}OH$), non-radical molecules such as hydrogen peroxide (H_2O_2) and singlet oxygen ($^1O_2$) are included (Sharma, et al. 2014). Having such a high chemical reactivity explains the negative effect on biological activities as well as cells. Once the level of ROS in the system exceeds a defense mechanism it is considered to go into a state of oxidative stress. Methods in which to enhance the performance or creation of ROS include redox cycling, interactions with electron transport chains, and photosensitization. Along with over production of ROS and the negative effects of ROS, further studies are trying to relate to their ability to alter its function to signaling pathways and be able to utilize ROS as messenger molecule (Di Giulio and Meyer 2008).

Ionizing Radiation

Ionizing radiation is the process in which radiation carries enough energy from an atom or molecule to a free electron. There is non-ionizing and ionizing radiation, the first one being negligible and the later being extremely harmful. Radiation is energetic subatomic particles, atoms moving at high speeds and electromagnetic waves. Both ionizing and non-ionizing can occur naturally or artificially. Ionizing radiation is the one to be aware of for its harmful properties. Sun bathing or eating a microwave dinner are examples of non-ionizing circumstance that should not bring concern. Cosmic rays, gamma rays, and x-rays fall under the category of ionizing radiation and in abundance can be fatal.

Oxidative Stress

The variety in which oxidative stress manifests itself into a system is boundless. It is an imbalance caused by the presence of ROS and the cell is unable to counterbalance. This can result in damage to one or more biomolecules such as lipids, DNA, RNA and proteins. These reactions can alter intrinsic membrane properties like fluidity, ion transport, loss of enzyme activity, protein cross-linking, inhibition of protein synthesis, and DNA damage, ultimately resulting in cell death (Sharma, et al. 2014). "Apart from affecting the cellular proteins, lipids, and DNA, ROS have a very crucial role in inducing apoptosis in the mitochondria. When there is increased oxidative stress in the cell, it may either result in the apoptosis or necrosis of the cell, depending on the extent of oxidative stress" (Nalabotu and Blough 2013).

Lipid Peroxidation

Lipid peroxides are an unstable marker resulting from oxidative stresses that decompose to form complex, reactive by-products that can damage proteins and DNA. "Lipid peroxidation a well-defined mechanism of cellular damage in either plants or animals that occurs in vivo during the aging in certain disease states" (Lipid Peroxidation n.d.). There are three distinct stages noted in lipid peroxidation, initiation, progression, and termination. Increasing levels of oxidative stress or ROS in a system could be the source of an increase in lipid peroxidation (Sharma, et al. 2014).

Toxicity

Toxicity, simply put, is the degree in which one substance is harmful to another. Factors relating to the cause of toxicity in a biological system (relating to the toxicity of water, plants, animals, and humans) are a widely researched in today's scientific community. All topics in science have limitless opportunities for exploration. Each with different properties and a biological system they are related to in some way. The increase of nano-materials in the industry and their release of nanoparticles into the environment have been of recent interest. Nalabotu and Blough noted that while animals and humans have been exposed to naturally occurring nano-materials, engineered nano-materials is what has been posing a toxic threat. Ge Ling noted that previous works have proven a toxic effect from nC60 on bacteria, human cell membranes, and aquatic conditions (Jing, et al. 2014).

Electromagnetic Spectrum

Light is electromagnetic radiation consisting of particles and waves with different consequences as it falls on a substance. The light can be reflected by a substance, absorbed by the substance or at certain wavelengths (nanometers) are absorbed and the remaining then gets transmitted or reflected. Light can be directly related to colors and the color that is "seen" or transmitted is the complimentary color of that color being absorbed. If a sample were to absorb all wavelengths the color would appear black; the opposite will happen if no wavelengths are absorbed; it will appear colorless. The visible light spectrum is but one small-scale example of the electromagnetic spectrum. When dealing with colorless substances ultraviolet and infrared spectrophotometric methods are better suited (Lloyd, Chen and Mycek 2014). Ultraviolet-A having wavelengths between 320 and 400 nm, will be the source of light throughout the following study.

Spectrophotometry

The electromagnetic spectrum proved that all chemical compounds absorb, transmit or reflect light over a specific range of wavelengths. Spectrophotometry is the quantitative measurement of the reflection or transmission properties of a material as a function of λ, representing wavelength (nanometers). This method is widely used in areas such as chemistry, biology, physics, etc. for quantitative analysis. Atomic emission spectrophotometry and atomic absorption spectrophotometry are two variations of spectrophotometry. Atomic absorption is when an atom absorbs certain wavelengths from the electromagnetic radiation (not necessarily in the visible spectrum).

Atomic absorption is when atoms absorb the wavelength the energy will remain constant given radiation. Whereas the atomic emission is once an atom has been given energy or a light source and has excited itself to a higher state. Given the short lifespan of the excited state, the atom will release the energy to return to the ground state, called the "relaxation" period. Both absorption and emission spectrum on any given compound is unique, making it helpful to determine the identity, concentration or amount of radiation undergone for a given sample (So and Dong 2012).

Photochemical Reactivity

A photochemical reaction is any type of chemical reaction that occurs after absorption of light rays. This comprises each type of light including ultraviolet, infrared, and visible. Light rays cause an excitement in atoms and molecules; some of the electrons are shifted to a higher energy level resulting in more reactivity.

When comparing a light reaction to that of thermal energy singularly, the reactions made can follow different routes between the two. Pertaining to the photochemical aspect of reactions, some of the routes that it follows result in the production of free radicals. Free radicals assemble under the category of ROS; this topic will be covered in more depth in the Reactive Oxygen Species section. Producing free radicals can often times trigger and thus sustain chain reactions.

A chain reaction is a sequence of reactions where one reactive product or byproducts cause additional reactions. Such reactions can be of a positive or negative nature. A thermodynamic non-equilibrium environment is where the system can release energy or an increase in entropy. This is a commonplace where chain reactions have experienced materialization.

High Performance Liquid Chromatography

Chromatography branches into two categories, analytical and preparative which correlate to the scale of separated analytes. Analytical chromatography is used to determine the existence and concentration of analyte(s) in a sample. Preparative chromatography is used to purify sufficient quantities of a substance for further use, rather than analysis. These proceedings done in the following experiment were strictly analytical. The ultra-high performance liquid chromatography (uHPLC) adheres similar functions only at a larger scale. The standard column particles size range from 3 μm to 5 μm. There also is a jump in pressure through the system, 400 bar to a pressure of approximating 100 bar. The main advantages to these systems are speed, sensitivity, and they rely on smaller volumes of organic solvents. When running trials with pressures exceeding 800 bar the columns degrade quicker.

Degradation Rate

Degradation is only one piece of information that can be found through HPLC testing. It is the breaking down, or the reduction in the quality and condition of a given substance. A chemically driven example could be the degradation of complex compounds such as a protein or polymer. The degradation rate is the rate in which a substance degrades over some period of time. The cleanliness of water sources is impertinent and free from harmful attributes. The rates in which substances degrade over time in a given solution are detrimental in knowing. This will help determine the substances that are most harmful and have the longest life expectancy, in turn will properly allocate the necessities at hand for purification.

Methods

Preparation of nC$_{60}$ sample

A solvent exchange process was carried out to obtain the nC$_{60}$ solution. The solution of 400 mg$\cdot$L^{-1} C$_{60}$ in toluene was prepared by dissolving 40 mg of solid C$_{60}$ powder into 100 mL of toluene. The two sealed jars of solution sat overnight in a thermostatic shaker to ensure that the C$_{60}$ completely dissolved into the toluene. The solution reached a dark purple color indicating that the powder was fully dissolved. After 400 mL of ultra-pure water was added, a total solution of 500 mL had been accumulated.

The jar containing the solution was sealed with parafilm. The jar was placed in an ultrasonic machine for 48 hours so that the C$_{60}$ could gradually enter into the aqueous phase. Every three hours the water was drained and new water was filtered into the ultrasonic machine, to prevent the temperature from rising above 25°C.

It took five, nine-hour lab days to complete the ultrasonic portion of the suspension; the machine was shut down at nights since it was unmonitored. The ultrasonic process was resumed immediately the following morning until the full 48 hours were complete.

Figure 3: Rotary Evaporator (Photo taken in Shanghai Jiao Tong Minhang Campus Water Pollution Control Laboratory)

A rotary evaporator (Buchi, Rotavapor System; Rotavapor R-215; Vacuum Controller V-850; Vacuum Pump V-700, Switzer- land) shown in **Figure 3** was used to extract the toluene from the mixture. When the evaporation of the toluene was complete the remaining aqueous solution was vacuum filtered through a 0.22 μm nylon syringe membrane.

Characterization of nC_{60}

The mass concentration of nC_{60} was measured through a two-step destabilization extraction process. Using 1 mL of 0.1 M of Magnesium Perchlorate $(Mg(ClO_4)_2)$, 2 mL of nC_{60} was extracted with 2mL of toluene. Three separate vials with the two-phase system were sealed, placed on a magnetic stirrer for approximately 2 hours, and then placed in a freezer to solidify the solution.

The unfrozen organic component was extracted, put into a 1 cm crystalline cuvette to measure the absorption spectrum at 336 nm with a Molecular Fluorescence Spectrophotometer (RF-5301PC, Shimadzu, Japan). As Ge Ling noted, the 336 nm is the length at which C_{60} has its maximum specific absorption peak. The absorption was observed and recorded three times for each vial of the solution. The concentration of nC_{60} was calculated through Equation1; the y-variable equaled the absorption recorded, the x-variable represented concentration. The 0.0676 represented the slope of known absorption and concentrations given from previous research by Ge Ling. The concentration for the nC_{60} is shown in **Table 1**.

$$y = 0.0676x \qquad\qquad (1)$$

Standard Curve

A standard curve shows the relationship between two quantities. Its functionality is to determine the concentration value of an unknown quantity by using the one that is more easily measured. The graphical relationship between the known value along the x-axis, and the assay along the y-axis is plotted. A line is drawn to best represent the curve of the data plotted. The equation to that line is the standard curve.

Table 1: Calculating the Concentration of nC_{60}

	Vial 1 Absorption	Vial 2 Absorption	Vial 3 Absorption	Average Absorption	Concentration (mg/L)
1	0.067	0.205	0.297	0.0637	0.9423
2	0.057	0.251	0.304	0.2050	3.0325

Dynamic Light Scattering

The Dynamic Light Scattering (DLS) (DLS Delsa 7M Nano C Particle Analyzer, Bechman, USA) analysis was one of two prevalent assessments with nC_{60} prior to this study. Dynamic light scattering (DLS) can also be referred to as photon correlation spectroscopy. This particular technique is non-invasive and measures the size and size distribution of a particle or molecule. This method has the advantage in being able to analyze a sample that contains a broad distribution of species or multiple molecular masses. The case at hand was a perfect example for when to use DLS given its aggregate state. DLS is used to detect extremely small amounts of species that gave a higher mass, <0.01% in most cases.

Choosing this method over others may relate to the short duration and almost completely automatized for routine measurements. Most systems operate at a 90° angle and generally use a red light (675 nm). Theory explains that light scattering is when light imposes on matter; the electric field of light then stimulates an oscillating polarization of electrons in a given molecule. "Analysis of these intensity fluctuations yields the velocity of the Brownian motion and hence the particle size using the Stokes-Einstein relationship" (Dynamic Light Scattering (DLS) 2016).

The PhD candidate Ge Ling at the School of Environmental Science and Engineering, at Shanghai Jiao Tong University continued and extensively researched nC_{60} aggregates for a better understanding of its characteristics. To analyze the particle size distribution and Zeta potential of nC_{60} samples dynamic light scattering was performed. The samples were prepared in triplicates and ranged from a pH of 1 to 9. Temperature was monitored at 25°C for all measurements. The particle size was measured five times and ten times for electrophoretic mobility (Jing, et al. 2014). Preparation methods to obtain the nC_{60} aggregate solution was a replication of works by Ge Ling. Ge Ling noted that the DLS was carried out with nC_{60} aggregates alone and in the presence of Poly-ethylene glycol octylphenol ether (TX100) micelles.

Transmission Electron Microscopy

Transmission electron microscopy (TEM) operates by using electrons rather than light. When analyzing data from a light microscope there is a limitation by the wavelength of light. Using the electrons as a light source allows for a resolution that is a thousand times better than with a light microscope. Objects are seen in the order of a few angstrom (10^{-10} m).

TEM operates by using electromagnetic lenses to create a very thin beam where the electrons are focused. The beam passed through the sample and then the electrons disappeared from the beam after scattering. Shadow like images depicting the different parts of the sample are shown pertaining to the density and to determine the particle size and morphology of nC_{60}; transmission electron microscopy (TEM) (JEM-2100, Japan Electronics Corporation, Japan) post research analysis was performed by Ge Ling. To prepare the specimens for TEM a droplet of the nC_{60} solution was dried on a copper grid overnight in a vacuum drying oven set at 25°C (Jing, et al. 2014).

Batch Experiments tested nC_{60} in different aquatic conditions

Batch experiments were carried out to identify nC_{60}'s physiochemical properties and how their potentially effects on a biological system. Similar methods were adopted from Ge Ling with minor variations. 0.0825 g of Terephthalic Acid was dissolved in NaOH to achieve a final TA concentration of 10 mM, 30% H_2O_2 formulated for a final concentration of 30 mg/L. pBS (NaH2PO4*2H2O+Na2HPO4), Sodium Chloride (NaCl) and the nC_{60} aggregate solution were the key components in the experiments being analyzed by spectrophotometry.

TA and 4-chlorobenzoic acid (pCBA) are both ·OH scavengers (Kanazawa, Furuki, et al., Measurement of OH Radicials in Aqueous Solution Produced by Atmoshpericpressure LF Plasma Jet n.d.). They do not react with other radicals in a system. TA traps the OH and emits fluorescence at 425nm. Figure 4 shows TA's chemical structure and its correlation with OH.
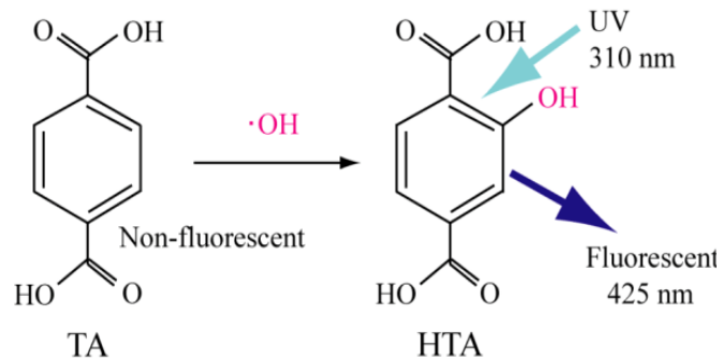
Figure 4: HTA formation through OH production

Ultraviolet-A Irradiation

The photoreaction equipment or UV reactor had six-4-W black light blue lamp (BLB lamps, Philips TL4W, Shanghai, China). Time allotments ranged from 0 to 140 minutes for varying solutions to undergo UV-A irradiation.

Spectrophotometry

The Molecular Fluorescence Spectrophotometer shown in Figure 5 was an RF-5301PC (Shimadzu, Japan). The excitation light was held at a constant wavelength of 315 nm. The emission scan range was set at 350-600 nm; the excitation slit width was set at 5.0 nm and the emission slit width was set at 5.0. Samples were pipetted into the 1 cm, square, non-fluorescent cell, or cuvette, and placed into the sample compartment. All specifications for the fluorescence spectra were held constant for both quartz and dark vial testing.

Figure 5: Molecular Fluorescence Spectrophotometer RF-5301PC (Shimadzu, Japan)

Fluorescence

Fluorescence is a photon emission process determining the measurement of fluorophores and their concentration during the exposure to external radiation. A fluorophore is the polyatomic fluorescent molecules themselves (So and Dong 2012). When a molecule that is at ground state absorbs a photon of excitation light the electrons may be raised to a higher energy and vibrational excited state. Taking no time for the reaction itself there is sometimes a vibrational energy loss from surrounding factors bringing it back to the lowest excited singlet state. The electrons are then able to settle back to ground state where there is a simultaneous emission of fluorescent light (So and Dong 2012). The light intensity emitted by a fluorescent material is dependent on the concentration of that material, making it important in quantitative analysis (Lloyd, Chen and Mycek 2014).

Quartz Vials

Quartz cylinders allow for fluorescence to travel through their sides, which then generates photochemical reactions. By altering parameters such as pH, concentration, ionic strength, and aggregate size of nC_{60} we were able to determine the influence on the production of free radicals by measuring it with spectrophotometry.

A magnetic stirrer was placed at the bottom of each cylinder and the cylinder was positioned on the magnetic stirring machine that was located inside the fluorescence machine or UV reactor. The timer was set to twenty minutes and the UV reactor was turned on. The three cylinders were removed from the reactor; a sample of approximately 2.75 mL was retrieved with a micropipette and released into the 10 mm square cuvette. The cuvette was placed into the spectrophotometer; a reading of the Absorbance Spectrum (abs vs. λ) was taken and recorded. The cuvette was rinsed with ultrapure water (ultra-purified to > 18 Ω) produced by a water filtration system (HtecH, Master-E, Japan) after testing each of the three solutions at each time interval.

Dark Vials

For the control scenario for the fluorescence detection experiments, dark vials were substituted for the quartz vials and a magnetic stir plate was used in the place of the UV reactor. The first time interval was at 20 minutes and a sample of approximately 2.75 mL from each solution were retrieved using a micropipette and placed into the 1 cm cuvette. The cuvette was placed in the spectrophotometer; a reading of the Absorbance Spectrum (abs vs. λ) was taken and recorded. The solutions were placed back onto the magnetic stirrer for another 20 minutes. Time allotments for this experiment proceeded for 20 min increments for a total of 100 minutes. The absorption for each solution was obtained at each time interval.

High Performance Liquid Chromatography

The High Performance Liquid Chromatography (HPLC)(Shimadzu LC-2010A Shanghai, China) used two solvent mixture phases. Standard high performance liquid chromatography (HPLC) is when an analyte is pumped into a solvent through a column with chromatographic packing material at high pressures. The analyte is the sample mixture at hand and the solvent is known as the mobile phase. The chromatographic packing material is also known as the stationary phase. HPLC is widely used in the scientific industry for applications including environmental, pharmaceutical, and chemical. For an HPLC analysis the injector is used to introduce the analytes to a fluent stream. The solvent, mobile phase is where the liquid is delivered under high pressure (up to 400 bar (4×10^7 Pa)) to ensure a constant flow rate. Lastly the stationary phase, stable due to location of hardware, is packed into a column capable of withstanding high pressures to influence the separation.

Base Solutions

In the chamber for two solvents 50% methanol and 50% 0.1 M pBS ($NaH_2PO_4 2H_2O$ + NaH_2PO_4) were used. The temperature was set at 40°C with a flow rate of 0.8 mL/min through the Agilent eclipse plus C_{18} column (4.6 mm x 250 mm, 5 µm). The wavelength was set to 234 nm. The HPLC was carefully controlled to the proper conditions. The method phases of 50/50% and the remaining conditions were saved to the HPLC hard drive for future procedures.

Phase A, methanol and phase B, 0.1 M pBS were poured into large glass jars with a screw on lid and then laced into the ultrasonic machine for five minutes with the lids slightly loosened. The appropriate lids were attached to the phase A and phase B jars and each phase was purged to remove residual bubbles from the aqueous solutions. A baseline of zero was achieved after running the machine for approximately four hours. The HPLC logged the retention time, area under the curve and height under the curve of each sample; data used to calculated degradation rate constants.

Sample Solutions

Fresh H_2O_2 was prepared prior to pCBA testing; 450 μL of 30% H_2O_2 was diluted with H_2O to achieve total volume of 100 mL. The final concentration of H_2O_2 is equal to 1.5 g/L. 4-chlorobenzoic acid (pCBA) was 3 mg of pCBA was dissolved in 100 mL of pure methanol. UV reactor was used to amplify or reestablish, the ability for free radical production. Time allotted for solutions ranged between 0 and 140 min and are displayed in **Table 2** detailing the solutions being examined.

Six different samples were developed with minor variations between each solution. Having only three quartz cylinders, solutions were divided into two sets of three solutions. The first listed as mentioned in Table 12 of the Results sections where solutions and all raw data are included in Appendix B. Prior to UV-A irradiation three vials from each solution were taken as a baseline. Aliquots were extracted with a syringe and filtered through a 0.22μm polytetrafluoroethene filter into 2 mL vials. A magnetic stirrer was placed at the bottom of each cylinder; the cylinders were set on the magnetic stir plate inside the UV reactor. The UV reactor was turned on and the timer was set for 20 minutes.

The first nine vials were placed in the HPLC tray, located behind the door on the front of the machine. The previously saved method with the desired conditions was opened, the HPLC was programmed to analyze the 54 vials and record the results to its hard drive. The three cylinders were placed back into the UV reactor both resumed power simultaneously. The timer reached 40 minutes, the UV reactor was switched off and the process was repeated; three, 2 mL vials for each of the three solutions.

The time increased in 20-minute intervals until 100 minutes was reached. The finished sets of prepared vials were placed into the HPLC tray; each took eight minutes to analyze and to record its results. The HPLC carried out the evaluation of each vial unassisted; it recorded the three pieces of data previously mentioned.

The second groups of solutions were formulated. The original three 2 mL vials were placed back into the UV reactor and the timer was set for 20 minutes. The UV reactor was stopped at each of the 20-minute time intervals in order to grab the 3 vials per solution and place them into the tray. Then the solutions were placed back into the UV reactor and the process was repeated until all 54 vials were in the tray.

Results and Discussion

With strict time constraints during this case study only two methods of observations were tested and analyzed. Pre- and post-works done by PhD candidate Ge Ling with substantial evidence to better understanding the data collected (Jing, et al. 2014).

Dynamic Light Scattering

The mean size (Z-average diameter) of nC_{60} was found relative to 115 nm and with a sample pH of 7.31. As noted, the particle size distribution was relatively centralized and its polydispersity index was 0.134. The data collected showed an obvious relationship between aggregate size and pH value. Figure 6 depicts the diameter of an nC60 aggregate. Figure 7 showed the aggregate size increased drastically when the pH was below 3.8. With a pH greater than 3.8, the aggregate kept a consistent diameter of 115 nm (Jing, et al. 2014).
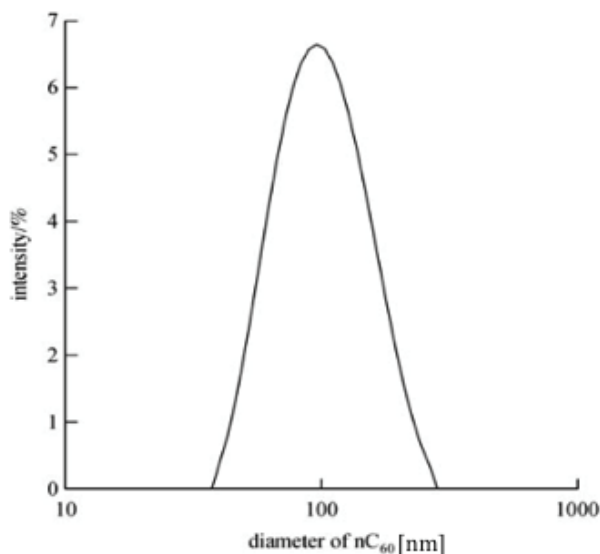
Figure 6: DLS characterization of nC_{60} (illustrates a graphical depiction of (Z-average diameter) (Jing, et al. 2014)
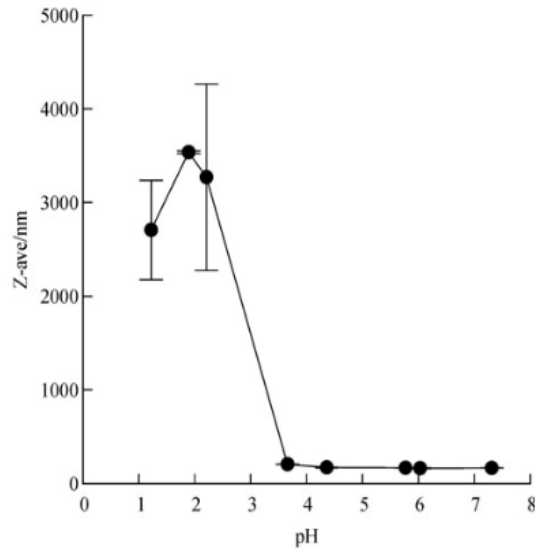
Figure 7: DLS analysis of strictly nC_{60} at varying pH levels (Jing, et al. 2014)

The nC_{60} suspension method remained constant for both studies; thus allowing for the assumption that the nC_{60} suspension utilized presently would portray similar traits with minor variations. In this study once suspension into toluene was complete the product was transparent and a brownish-yellow color suspended solution, nC_{60}.

Transmission Electron Microscopy

Ling assessed the shape and structure of the same nC_{60} samples with transmission electron microscopy. As discussed previously the shape and structure determine the type of fullerene in use and any affect it may have on a biological system. The aggregates were observed to be spherical and approximating 100 nm in diameter as illustrated in Figure 6. Figure 8 shows an image of the nC_{60}.
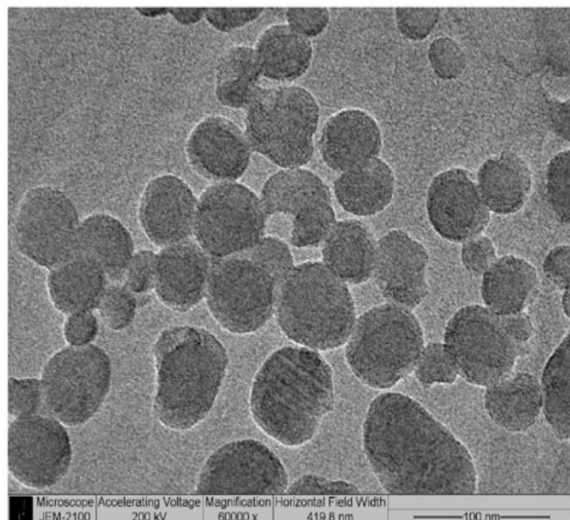
Figure 8: TEM image of nC_{60} (Depicts a grey scale image of nC_{60} shape) (Jing, et al. 2014)

Batch Experiments of nC_{60}

The contents for the various solutions used in each of the experiments are depicted in **Table 2** through **Table 11**. UV-A irradiation or magnetic stirring was performed as the reaction phase in each experiment. **Figure 9** though **Figure 18** below show the maximum intensities for each solution on the y-axes and the given time in minutes for the reaction phase on the x-axis.

Spectrophotometry

Spectrophotometry was the method for the measurement in fluorescence absorption, allowing the ability to witness the production or quenching of ROS. In this study the ROS being observed for is a hydroxyl radical (·OH).

Standard Curve

The nC_{60} aggregate solution previously formulated by Ling with the standard curve that depicts the measured concentration of the batch used in this study is shown in Equation 1 in the Methods: Characterization of nC_{60} section. Prior to the quartz and dark trials 3 separate vials of the nC60 were measured in the spectrophotometer.

Quartz Vials

Table 2 and **Table 3** demonstrate the contents that comprise each solution. All measurements remain uniform excluding the 200 mM pBS. The first three solutions retrieved 5 mL of pBS and 2 mL of pBS respectively. The different volume of the pBS acted as a buffer and was used to lower the overall pH of the solution prior to the UV-A irradiation.

The pH for every solution was noted before UV-A irradiation began and is also listed in each Table hereafter.

Table 2: pBS Initial Volume

Vials	TA (10 mM)	H_2O_2 (30%)	nC_{60}	pBS (200 mM)	H_2O	pH
1	4 mL	4 mL		5 mL	27 mL	7.45
2	4 mL	4 mL	13 mL	5 mL	14 mL	7.39
3	4 mL	4 mL	13 mL	5 mL	14 mL	7.30

Table 3: pBS Reduced Volume

Vials	TA (10 mM)	H_2O_2 (30%)	nC_{60}	pBS (200 mM)	H_2O	pH
1	4 mL	4 mL		2 mL	30 mL	11.93
2	4 mL	4 mL	13 mL	2 mL	17 mL	11.86
3	4 mL	4 mL	13 mL	2 mL	17 mL	11.87

Figure 9 shows the decrease in fluorescence, meaning there was a quenching trend on the production of hydroxyl radicals. Having a higher volume of pBS shown from the data in Table 2 created a significantly lower pH of the starting media of the solution. Contrasting data aid in proving the previous statement to be true, as the volume was lowered for the pBS buffer the pH made a drastic increase. The higher pH value in these sets of data allowed for the production of the free radicals illustrated by the fluorescence increase in Figure 10.
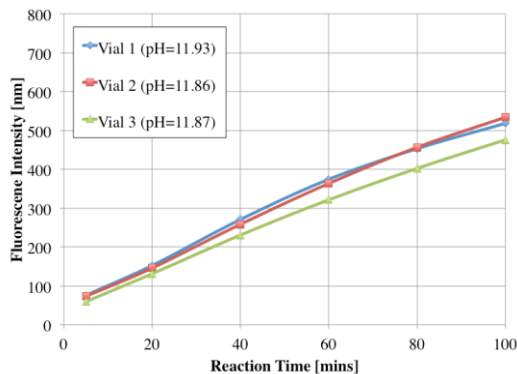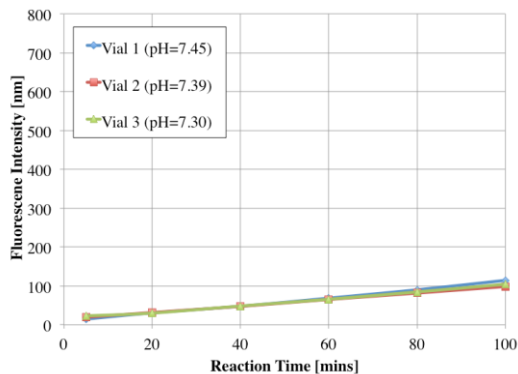
Figure 9: pBS Initial Volume Intensity   Figure 10: pBS Reduced Volume Intensity
(Altering the pH of the media to witness its effects on the production of OH)

In **Table 4** and **Table 5** the variable changed was the TA in the solution. Retaining the same initial concentration of TA (20 mM), the volume was altered; changing the final concentration of TA added to the solution. In **Table 4** it went from 4 mL and then was reduced down to 2 mL. These solutions were to demonstrate the fluorescence capabilities of TA once it has scavenged ·OH.

Table 4: TA Initial Volume

Vials	NaOH (100 mM) TA (20 mM)	H_2O_2 (30 mg/L)	nC_{60} (9.88 mg/L)	pBS (pH 7) (80 mM)	H_2O	pH
1	4 mL	4 mL		4 mL	28 mL	12.08
2	4 mL	4 mL	4 mL	4 mL	24 mL	12.11
3	4 mL	4 mL	16 mL	4 mL	12 mL	12.67

Table 5: TA Reduced Volume

Vials	NaOH (100 mM) TA (20 mM)	H_2O_2 (30 mg/L)	nC_{60} (9.88 mg/L)	pBS (pH 7) (80 mM)	H_2O	pH
1	2 mL	4 mL		4 mL	30 mL	8.36
2	2 mL	4 mL	4 mL	4 mL	26 mL	8.38
3	2 mL	4 mL	16 mL	4 mL	14 mL	8.39

As Figure 11 and Figure 12 depict a very obvious difference between the two trials. As the initial pH of the first 3 solutions were higher as well as the concentration of TA. Thus being able to promote the scavenging of ·OH and emitting its fluorescence. Figure 12 shows the counterstatement of a lower initial pH in the media and less overall TA the lower the production. With less TA its ability to scavenge and emit that fluorescence is decreased. Figure 12 still showed signs for an increase of ·OH toward the end of the reaction time, even if only a fractional amount.
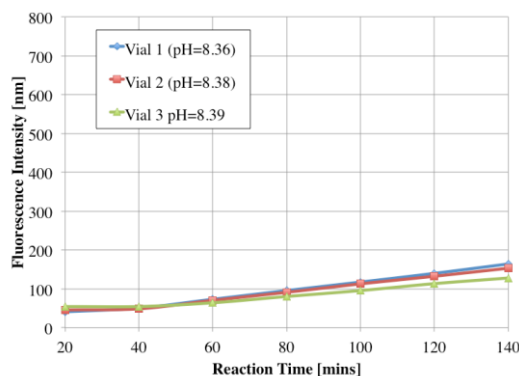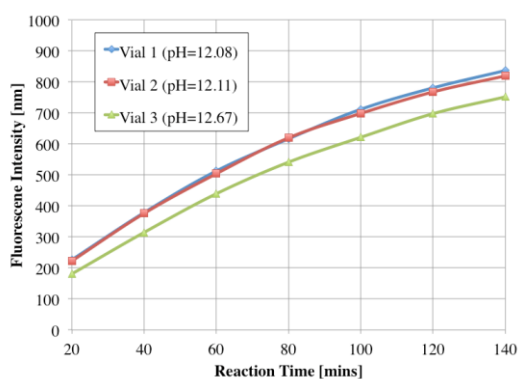
Figure 11: TA Initial Volume Intensity   Figure 12: TA Reduced Volume Intensity

(Without the fluorescence ability from TA the production of OH unnoticeable in less concentration)

Table 6 **and**

Table 7 show that NaCl (0.5 M) was added to each solution in place of pBS that was used in the previous trials. Table 5 shows the initial volume added to each of the three solutions was 4 mL. Table 6 displays the reduced volume at 1 mL. Adding NaCl altered the ionic strength of each nC_{60} solution without affecting the pH of the system.

Table 6: NaCl Initial Volume

Vials	NaOH (100 mM) TA (20 mM)	H_2O_2 (30 mg/L)	nC_{60} (9.88 mg/L)	NaCl (0.5 M)	H_2O	pH
1	2 mL	4 mL		4 mL	30 mL	11.23
2	2 mL	4 mL	4 mL	4 mL	26 mL	11.25
3	2 mL	4 mL	16 mL	4 mL	14 mL	11.26

Table 7: NaCl Reduced Volume

Vials	NaOH (100 mM) TA (20 mM)	H₂O₂ (30 mg/L)	nC₆₀ (9.88 mg/L)	NaCl (0.5 M)	H₂O	pH
1	2 mL	4 mL		1 mL	33 mL	11.30
2	2 mL	4 mL	4 mL	1 mL	29 mL	11.26
3	2 mL	4 mL	16 mL	1 mL	17 mL	11.24

From the tables it is observed that the volume difference in NaCl hardly altered the pH of each starting solution.

Figure 13 and Figure 14 show little to no consequence on the fluorescence intensity of these solutions. The fluorescence intensity increasing over time correlates to an increased level of ·OH being produced. The two figures also depicts that the alteration of ionic strength of a given solution is of little value when determining the production on · OH. Fluorescence intensity only increased noticeably for vial 1 in the second trial, by any noticeable amount. The vials with the largest concentration show the lowest amount of fluorescence. Supporting the claim that quenching takes place with the increase in nC_{60} remains apparent by the data. It can also be concluded from the data the production of those hydroxyl radicals is still taking place just at a slower rate.
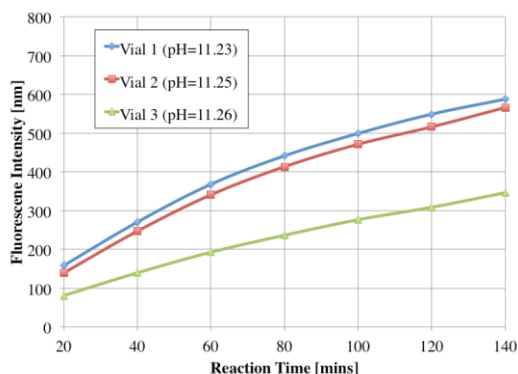
Figure 13: NaCl Initial Volume Intensity
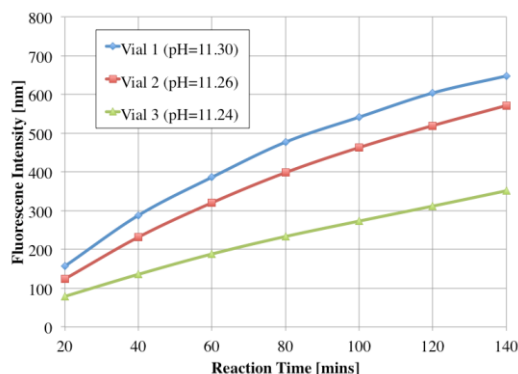
Figure 14: NaCl Reduced Volume Intensity

(Adding NaCl altered the ionic strength of each solution)

43

Table 8 and Table 9 alter the initial concentration of the TA component. Also these six solutions exclude a buffer, pBS and NaCl, entirely. The pH noted in Table 8 was the one exception from all previous pH measurements. It was recorded the subsequent day of UV-A irradiation. The initial concentration of TA alters between 20 mM and 10 mM respectively. The volume difference of 2 mL versus 4 mL does in fact finalize at the same concentration that is being added to each solution.

Table 8: TA Initial Concentration

Vials	NaOH (200 mM) TA (20 mM)	H_2O_2 (30 mg/L)	nC_{60} (9.88 mg/L)	H_2O	pH
1	2 mL	4 mL		34 mL	10.3
2	2 mL	4 mL	8 mL	26 mL	10.5
3	2 mL	4 mL	32 mL	2 mL	11.13

Table 9: TA Final Concentration

Vials	NaOH (200 mM) TA (10 mM)	H_2O_2 (30 mg/L)	nC_{60} (9.88 mg/L)	H_2O	pH
1	4 mL	4 mL		32 mL	12.87
2	4 mL	4 mL	8 mL	24 mL	12.89
3	4 mL	4 mL	32 mL		12.90

Figure 15 and Figure 16 show an increase in fluorescence intensity like many of the rest. As it correlates to the Figures seen above having the concentration of the TA being lowered it proves less fluorescence. Figure 15 values are slightly below that of Figure 11 given the increase of nC_{60} on the system. That data vs. this set has vial 2 and vial 3 at 4 mL and 16 mL compared to 8 mL and 32 mL respectively. Having doubled the intake of nC_{60} the results from Figure 11 had vial 1, 2, 3 measuring 900, 800, 750 nm respectively. While shown below in Figure 16 is the perfect counterpart for Figure 11 given all measurements being the exact replica except double the nC_{60}. This depicts that as long as the final concentration of the TA added to a given solution must be great enough to pick up that ·OH and emit fluorescence.
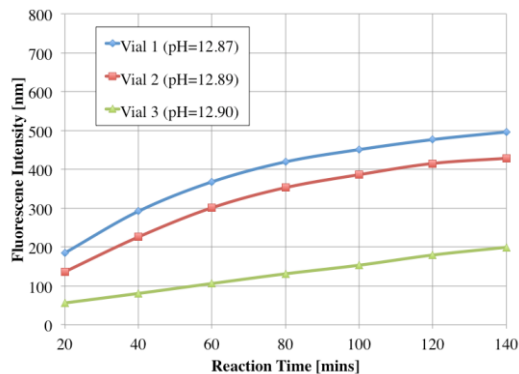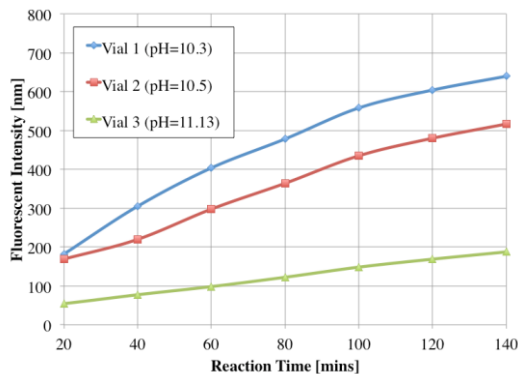
Figure 15: TA$_i$ Concentration Intensity   Figure 16: TA$_F$ Concentration Intensity

(Figures show the intensity without a buffer added to its composition)

Dark Vials

Table 10 and Figure 17 were the first set of control solutions, without the influence of UV magnetic stirrers and stir plates were put in place. Table 10 included each substance strictly by itself and pBS to show its fluorescence capabilities.

Table 10: Dark Vials Trial 1

Vials	TA (10 mM)	H$_2$O$_2$ (30%)	nC$_{60}$	pBS (10 mM) (pH=5)	pH
1	4 mL			36 mL	9
2		4 mL		36 mL	5.5-6
3	4 mL		13 mL	23 mL	9
4	4 mL	4 mL		32 mL	9
5	4 mL	4 mL	13 mL	19 mL	9
6			13 mL	27 mL	5.5-6

As Figure 17 shows there is almost zero change to the fluorescence measured from any of the six solutions. Having no UV-A irradiation in the system did not allow for the production of hydroxyl radicals in the trials exhibited in Figure 17. The data points shown below include a few that are slightly skewed, this is generally caused by poor pipetting, improper rinsing or residual material left in the cuvette that would also be a skewed data.
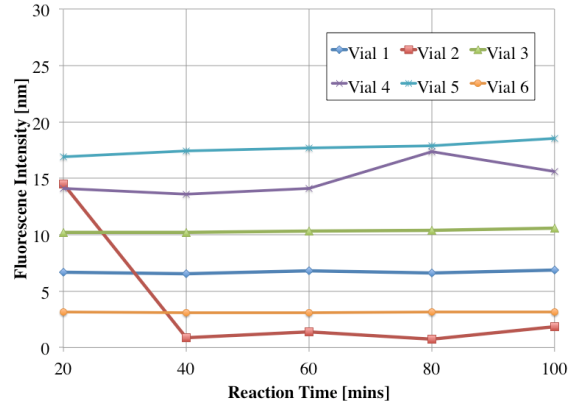
Figure 17: Dark Vials Trial 1 as control to show no fluorescence emission (no ·OH)

Table 11 and Figure 18 were in correspondence to the second set of the dark vial trials. Table 11 having the final concentration of the pBS listed beside the initial pBS showed an original trend. Stated previously the pBS was used as a buffer solution to intentionally lower pH values of each solution. In this circumstance hydrochloric acid (HCl) was also used as an additive. It helped to dilute the solution and lower the pH for vial 1 and vial 2 while keeping vial 3 the control having nothing.

Table 11: Dark Vials Trial 2

Vials	TA (10 mM)	H_2O_2 (30%)	nC_{60}	pBS (10 mM)	Final Concentration	HCl	pH start/finish
1	4 mL	4 mL		28 mL	7 mM	4 mL	8/8
2	4 mL	4 mL	13 mL	15 mL	3.75 mM	4 mL	8/8
3	4 mL	4 mL	13 mL	19 mL	4.75 mM		9/9

Figure 18 did not show the same effect as the first dark vial trials. Despite having no UV-A irradiation, Figure 18 showed a steady increase in fluorescence intensity once approximating 20 minutes of magnetic stirring and thereafter. In the final measurement on the fluorescence spectra taken the noted intensity for each vial was 180, 500, 610 nm respectively. Vial 2 and Vial 3 having the highest production of ·OH include the 2 lower volumes of pBS. Vial 1 has 0 mL of nC_{60} whereas vial 2 and vial 3 each had 13 mL. The generalized note prior to the dark trials was nC_{60} had quenching abilities on ·OH while undergoing UV-A irradiation. The magnetic stir plates had the opposite effect. The longer the reaction time being stirred the more ·OH production is reestablished.
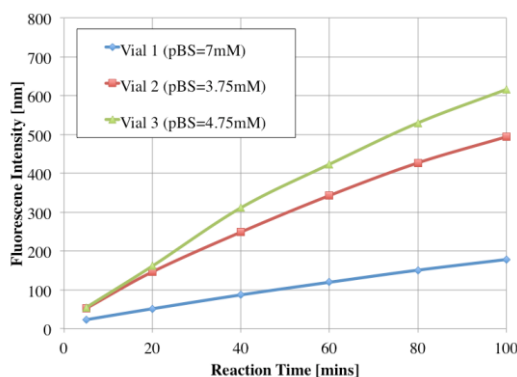
Figure 18: Dark Vials Trial 2 with alterations to initial buffer pH

Vial 1 hardly increased in intensity through the 100 min being stirred. Vial 1 not reaching over 200 nm and is affected by each of the factors against it. The high concentration of pBS, HCl and without the nC_{60} to generate additional photochemical reactivity. Despite those factors to deplete the pH Figure 18 illustrates that production of the radicals in vial 1 was greater than zero and over an allotted amount of time (min) it continues increasing very minimally. Found in the Appendix are all other miscellaneous trials using spectrophotometry as the method to measure the absorption of each solution.

High Performance Liquid Chromatography

Table 12 lists the solutions prepared for testing using the HPLC machine in Trial 1. Three vials of solution were tested and the three measurements for each time interval after UV-A irradiation were recorded in.

Table 12: HPLC Trial 1

Vials	pCBA (30 mg/L)	H_2O_2 (1.5 g/L)	nC_{60}	H_2O	pH
1	4 mL			36 mL	8.63
2	4 mL	4 mL		32 mL	9.32
3	4 mL	4 mL	13 mL	19 mL	9.02

Trial 1 and Trial 2 used the HPLC method post UV to detect for hydroxyl radicals and their behavior depending on each solution. The retention time, the area under the curve and the height of the peak were respectively documented for further analysis. Figure 19 illustrates the results of the average area under the curve for each solution at t (min). This data is inconclusive and more experiments altering the solutions and absolute precision in measuring the data may have looked differently. Appendix B includes the raw data for Trial 1 and Trial 2.
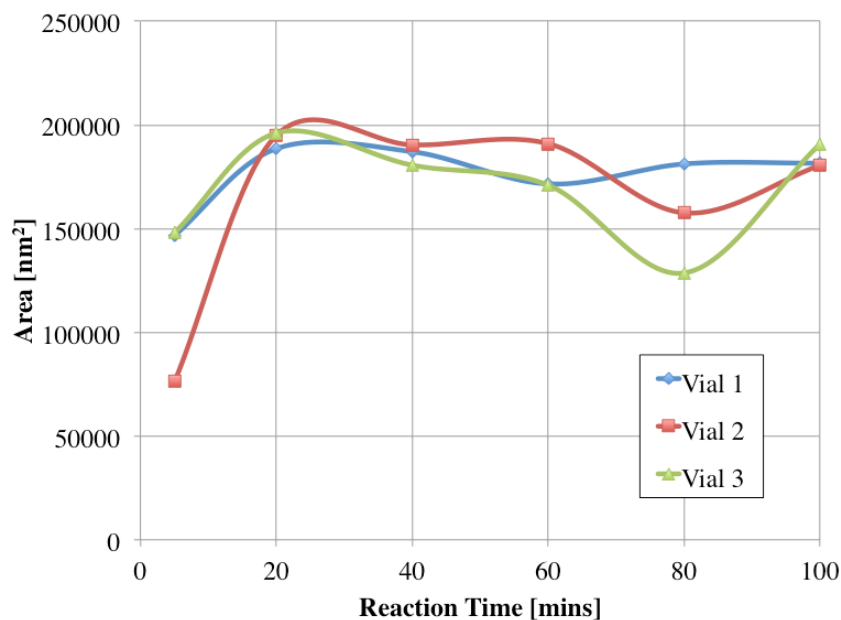
Figure 19: Area under the Curve in regard to time (min) using HPLC for analysis

Conclusions and Recommendations

Based upon the results obtained from the different trials involving the material in question, nC_{60} aggregates, the following characteristics were observed pertaining to its physiochemical and photochemical properties.

1. The average size of the nC_{60} aggregates in diameter was varied with pH, as the pH was greater the smaller the average size of each aggregate cluster became.

2. The pH of the aqueous solution had a tremendous effect on the fluorescence intensity, the greater the pH of the media the greater the production in $\cdot OH$.

3. Altering the ionic strength had no significant effects on the ability to quench or promote hydroxyl radicals ($\cdot OH$) formation.

4. UV-A irradiation and continuous movement showed an increase in the production of $\cdot OH$ witnessed by the fluorescence intensity rising as a function of time (min).

There are a significant number of experiments and different measurements for analysis that will either provide more support or deny these characteristics of nC_{60} and its environmental influences. As noted in previous works, solvent exchange methods to obtain nC_{60} aggregates like in this current study allow a greater margin of error. While the method to perform is kept consistent, the factors of the system are not. Whether by altering the ionic strength, pH, aggregate size, or concentration of initial C_{60} used, outside factors such as aqueous pH, reaction time, NOM and concentration of media added are vital to the final verdict of nC_{60} for a given solution.

The UV-A irradiation method was noticeably successful in illustrating the production of the OH and the outcome in different aqueous solutions. Since nC_{60} cannot generate the photochemical reaction like its former self-C_{60}, by adding it to a TA and H_2O_2 it ensured the production of OH and the capability to witness it by measuring the fluorescence spectra. For our non-uv method with the magnetic stirrers and magnetic stir plate it also showed an upward trend of fluorescence as the more time (minutes) passed.

In each set of the alterations made to the solutions, the ones having the greater quantity of nC_{60} did show a reduction in the fluorescence spectra. The reduction in intensity demonstrated that the more nC_{60} added to a system, the more quenching will be observed (to some extent). However, it quenches the production of radicals not demolishes it; therefore the solution can be altered depending on the desired outcome and prior conditions.

Many case studies have shown the production of hydroxyl radicals or any other free radicals as being a major cause in cell damage, early aging, among other less desirable outcomes. Sometimes even death can result. The data collected in this study it further shows that nC_{60} is much too diverse of a molecule to state any findings as being concrete. A distinct answer as to whether nC_{60} does or does not cause toxicity in a system is not possible. The results from current studies are so variable amongst them there is no concrete answer at this time for nC60 in general.

It is suggested that a larger batch of nC60 correlated to the amount of experimentation to be done be made, rather than small quantities. The need to make more nC60 solution rather than having the exact duplicates throughout specific tests will ensure the accuracy of the results on the effects of that nC_{60}. It could also potentially pin point the factors that cause the results for previous studies. Also there area at least five unexplored surfactants within the solutions that have both hydrophobic and hydrophilic qualities that can be further studied to understand their effects on nC_{60}. Altering the pH, concentration and reaction time are some of the processes to alter the solution that should remain constant for a feasible comparison. However the pH should be tested in a wider range, and rather than just two different concentration, five different initial concentration, and five final concentrations of nC_{60} should be examined.

The UV-A irradiation demonstrated the photochemical reaction in the current study where the dark vials had one promising trial and the other flat line results as seen in **Figure 17**. The second trial for dark vials (**Figure 18**) demonstrated that there was still the ability for the system to reestablish that capability in producing hydroxyl radicals. In **Figure 18** it can be seen that the vial with the most intensity also had the most nC60 present in the solution. This was the one particular case during the entire study, the rest of the study showed the opposite trend. This further demonstrates that additional research and analysis is essential for a better understanding of nC_{60} in altered types of solutions and the adverse and inverse effects of it on a biological system.

Engineering Project Design

This portion provides a feasible design for a UV reactor column in place of the previous chlorination phase for disinfection. As observed in the foremost experiments inflicting UV radiation to the proper system it will generate hydroxyl radicals (OH). Injecting the water with nC_{60} aggregates measuring as it is released through the UV reactor column. Initiated the creation of hydroxyl radicals and stimulated an OH chain reaction leading to the elimination of residual organic matter.

This is a design for a full-scale treatment option involved in a water clarification process. The Upper Blackstone Wastewater Treatment Facility provided background information with daily flow rates (Q), effluent and influent rates pertaining to organic matter. This design took the place of chlorination; this particular plant was the perfect candidate as it is the local source for nearly all water usage, residential to industrial.

Blackstone having a maximum flow rate of 19,000,000 gallons/day (0.832 m^3/sec) and high levels of contaminated water continuously flowing through, it is imperative that before any discharge occurred the proper treatments and results were met. Figure 20 showed the flow plan in which UV reaction was proposed for this system once exiting the tank from the preceding step in the treatment process.
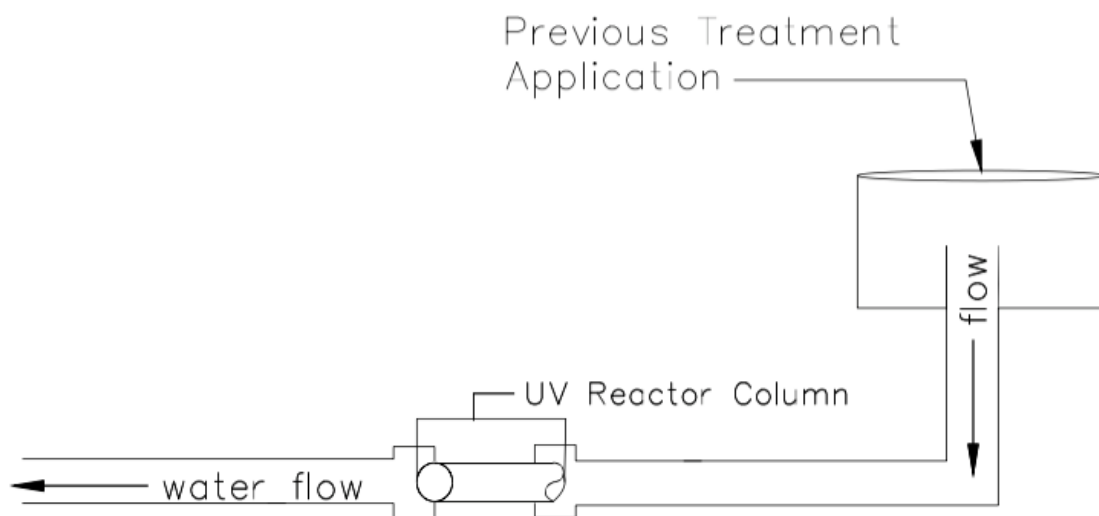
Figure 20: Water Flow from post to release from UV reactor

Piping between treatment processes in the system utilized Polyvinyl Chloride (PVC) material; it is a cheaper, durable material and less risk for corrosion without HCl involved. The UV reactor column is comprised of stainless steel with 3 UV bulbs sealed in a quartz sleeve around the outside layer of the UV reactor column. Quartz was chosen to allow the transmittance of fluorescence to pass through to the water, one key to producing OH as witnessed in this study.

Using Q at 0.832 m³/s, set the desired velocity (v) to 2.5 m/s, the cross sectional area of the column 0.333 m² and the surface area of the column 4.084 m². Aiming for a 99.99% removal rate of organic matter the standard UV usage was noted as being 60 mJ/cm². UV reaction time converted into kilowatts per day (kWh) was found and organized by cost to see if this design is worth the investment. Figure 21 is a close up and detailed image of the UV reactor being proposed. Followed by the calculations to transfer energy requirements into an actual cost. The standard removal amount from UV reaction is 600 J/m² which is converted to find the intensity required. The average cost per kWh is at a current rate of $13.20.
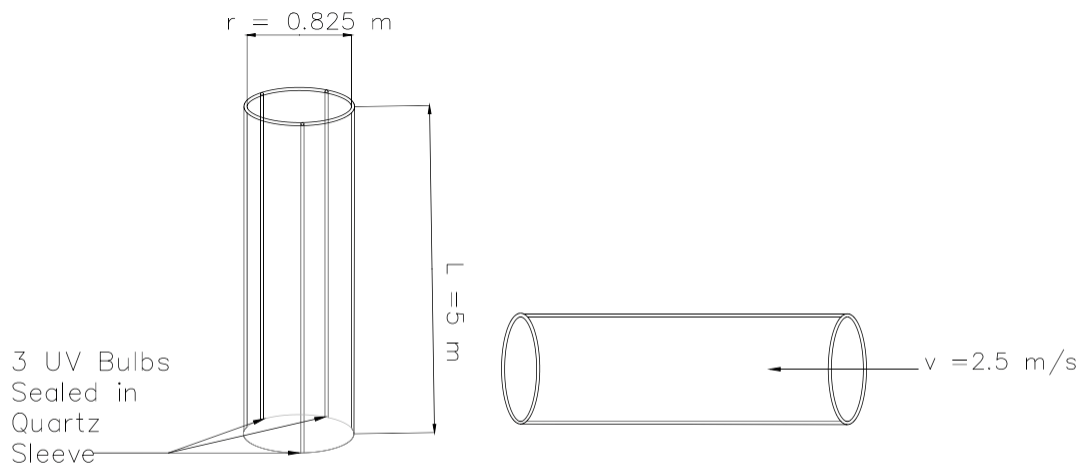
Figure 21: Detailed Layout of UV Reactor Column

Energy Requirements converted to Cost:

$$UV\ Reactor\ Dose\ =\ Intensity * reaction\ time$$

$$Intensity = Dose/Time$$

$$Intensity = \frac{600\frac{J}{m^2}}{5\ sec}$$

$$Intensity = 120\ Watts/m^2$$

$$Surface\ Area\ of\ Column = 2\pi r * L$$

$$Surface\ Area\ of\ Column = 2\pi(0.325\text{m}) * (2m) = 4.084\ m^2$$

$$Power\ Needed\ (Watts) = Surface\ Area\ of\ Column * Intensity$$

$$Power = 4.084\ m^2 * 120\ W/m^2$$

$$Power = 490.08\ W = 11.762\ kWh$$

$$Cost = Power\ (kWh) * cost/kWh$$

$$Cost = \$155.26\ /day$$

Table 13: Power Converted to Cost for Production

	Daily	Annually
Operating Reactor Cost	$155.26	$56,668.93
C_{60}	$135,071.00	$ 49,300,914.86
Reactor Initial Cost	$100,000.00	
Pipe Initial Cost	$297.26	

The cost being $155.26 per day to operate the reactor column estimates $56,668.93 dollars annually. When taking into consideration that the plant already has 98% as a removal rate of NOM. Tacking the total cost to switch and re-rout the preexisting pipes, installing the reactor and cost for nC_{60} itself to generate the radicals and maintain the required levels prior to discharge prove to be far greater an expense than the current method. Until a more cost effective method is found to generate UV radiation within a large-scale treatment plant maintaining the original disinfection by HCl spectacles to be the wiser option. Future investigation using the same design only at smaller scales could prove less financially demanding given that less pure C60 would be required annually bringing that $49 million dollar cost down. (Zoro, 2011-2016) (Atlantic Ultraviolet Cooperation, 2016)

Works Cited

A Cleanier Healthier Environment. (2007-2008). Retrieved 2016, from http://www.cvwrf.org/brochure/page17.php

Acero, J. L., Stemmlet, K., & Gunten, U. v. (2000, January 7). Degradation Kinetics of Atrazine and Its Degradation Products with Ozone and OH Radicals: A Predictive Tool for Drinking Water Treatment. *Environmental Science and Technology, 34*(4), 571-597.

Andrievsky, G., Klochkov, V., Karyakina, E., & Mchedlov-Petrossyan, N. (1999, February). Studies of aqueous colloidal solutions of fullerene C by electron 60 microscopy. *Chemical Physics Letters, 300*(3-4), 392-396.

Atlantic Ultraviolet Cooperation. (2016). *Sanitron Equipment*. Retrieved from Buy Ultraviolet: http://buyultraviolet.com/ProductDetails.aspx?item_no=24-2524A1&CatId=7e31383b-aa77-4c94-b900-2be83d25fbd0

Baun, A., Sorensen, S., Rasmussen, R., Hartmann, N., & Koch, C. (2008). Toxicity and bioaccumulation of xenobiotic organic compounds in the presence of aqueoussuspensions of aggregates of nano-C60. *Aquatic Toxicology*, 379-387.

Beltran, F. J. (2003). Kinetics of the Ozonation of Wasterwaters. In F. J. Beltran, *Ozone Reaction Kinetics for Water and Wastewater Systems.*

Beltran, F. (n.d.). Kinetics of the Ozone–UV Radiation System. In F. Beltran, *Ozone Reaction Kinetics for Water and Wastewater Systems.* Taylor & Francis Group.

Best Rank. (2004-2016). *Lipid Peroxidation*. Retrieved 2016, from http://www.cellbiolabs.com/lipid-peroxidation

Biological Wastewater Treatment with Activated-Sludge Process. (1998-2016). Retrieved 2016, from http://www.lenntech.com/wwtp/wwtp-overview.htm

Birlouez-Aragon, I., Buschmann, C., Hashimoto, A., Kameoka, T., Kumke, M. U., Lakhal, L., . . . Saito, Y. (n.d.). Fluorescence. In M. Zude, *Optical Monitoring of Fresh and Processed Agricultural Crops* (pp. 251-377). Taylor and Francis Group.

Boundless. (2015). *Allotropes of Carbon*. Retrieved from
https://www.boundless.com/chemistry/textbooks/boundless-chemistry-
textbook/nonmetallic-elements-21/carbon-150/allotropes-of-carbon-582-3569/

Bruno, T. J., & Svoronos, P. D. (2010). High-Performance Liquid Chromatography. In T. J.
Bruno, & P. D. Svoronos, *Handbook of Basic Tables for Chemical Analysis* (pp.
137-203). Taylor & Francis Group.

Chen, Lin, Q., & Fan. (2014). Study on the advanced denitrification in biological aerated
filter upgrading. *Modeling and Computation in Engineering*, 301-306.

Clark, J. (2007). *HIGH PERFORMANCE LIQUID CHROMATOGRAPHY - HPLC*. Retrieved
2016, from http://www.chemguide.co.uk/analysis/chromatography/hplc.html

Di Giulio, R. T., & Meyer, J. N. (2008). Reactive Oxygen Species and Oxidative Stress. In R.
T. Giulio, & D. E. Hinton, *The Toxicology of Fishes* (pp. 6-1-6-52). Taylor & Francis
Group.

DiToro, J. A. (2012). *Removal of Taste and Odor Causing Compounds Using Ultrafiltration
Membranes.* MQP, Worcester Polytechic Institute, Worcester.

Dorsey, A., McClure, P. R., McDonald, A. R., & Singh, M. (2000). *TOXICOLOGICAL PROFILE
FOR TOLUENE .* Syracuse Research Corpoation.

Drury, C., Myrold, D., Beauchamp, E., & Reynolds, W. (2007). Denitrification Techniques
for Soils. In S. S. Analysis, *Carter, M.R.; Gregorich, E.G.;* (pp. 471-493). Taylor &
Francis Group.

Dunk, P. (2015). The C60 buckminsterfullerene formation process: new revelations after
25 years. *C60 Buckminsterfullerene: Some Inside Stories*, 1-27.

Dynamic Light Scattering (DLS). (2016). Retrieved 2016, from
http://www.malvern.com/en/products/technology/dynamic-light-scattering/

Fei, H., Ling, G., Bo, Z., Yun, W., Hao, T., Liping, Z., . . . Xiaojun, Z. (2014). A fullerene
colloidal suspension stimulates the growth and denitrification ability of
wastewater treatment sludge-derived bacteria. *Chemosphere*, 1-7.

Fernandez-Garcia, N., & Olmos, E. (2014). ROS and NOS imaging using microscopical techniques. In S. D. Gupta, & Y. Ibaraki (Eds.), *Plant Image Analysis Fundamentals and Applications* (pp. 245-264). Taylor & Francis Group.

G.V. Andrievsky, V.K. Klochkov, E.L. Karyakina, N.O. Mchedlov-Petrossyan. (1999, February). Studies of aqueous colloidal solutions of fullerene C by electron 60 microscopy. *Chemical Physics Letters, 300*(3-4), 392-396.

Gavrilyuk, A. (2013). Production of Atomic Photochemical Hydrogen and Photoinjection of Hydrogen in Solids . In A. Gavrilyuk, *Hydrogen Energy for Beginners* (pp. 11-1-11-41). Taylor & Francis Group.

Gnanasammandhana, M. K., & Zhang, Y. (2012). Rare Earth Nanomaterials in Fluorescence Microscopy. In T. T. Tan (Ed.), *Rare Earth Nanotechnology* (pp. 83-106). Pan Stanford Publishing Pte. Ltd. .

Halliwell, B. (n.d.). *Free Radical Reactions in Human Disease .* National University of Singapore.

Henry, K. M., & Sellers, K. (2008). Treatment of Nanoparticles in Wastewater. In K. Sellers, C. Mackay, L. L. Bergeson, S. R. Clough, M. Hoyt, J. Chen, . . . J. Hamblen (Eds.), *Nanotechnology and the Environment* (pp. 155-168). Taylor & Francis Group.

Hideg, É., & Ayaydin, F. (2014). Fluorescent ROS probes in imaging leaves. In S. D. Gupta, & Y. Ibaraki, *Plant Image Analysis Fundamentals and Applications* (pp. 265-278). Taylor & Francis Group.

How Hydroelectric Energy Works. (n.d.). Retrieved 2016, from http://www.ucsusa.org/clean_energy/our-energy-choices/renewable-energy/how-hydroelectric-energy.html#.Vx2FApMrJR6

How is ozone formed in the atmosphere? . (n.d.). Retrieved 2016, from http://www.esrl.noaa.gov/csd/assessments/ozone/2010/twentyquestions/Q2.pdf

Hyun, J., Chan-Ung, W., & Wonhee, J. (2009). Nano-C60 and Hydroxylated C60: Their Impacts on the Environment. *Toxicol. Environ. Health. Sci. Vol. 1*, 132-139.

Ionizing Radiation . (n.d.). Retrieved 2016, from http://chemed.chem.purdue.edu/genchem/topicreview/bp/ch23/radiation.php#top

Jing, H., Ye, Y., Ling, G., Bo, Z., & Yiliang, H. (2014). Behavior of aqueous stable colloidal nano-C60 aggregates exposed to TX100 micelles under different environmental conditions . *Front. Environ. Sci. Eng.* , 1-9.

Jung, H., Wang, C.-U., & Jang, W. (2009). Nano-C60 and Hydroxylated C60: Their Impacts on the Environment . *Toxicol. Environ. Health. Sci.* , 132-139.

Kanazawa, S., Furuki, T., Nakaji, T., Akamine, S., & Ichiki, R. (n.d.). *Measurement of OH Radicals in Aqueous Solution Produced by Atmospheric-pressure LF Plasma Jet.* Oita University, Department of Electrical and Electronic Engineering.

Kanazawa, S., Furuki, T., Nakaji, T., Akamine, S., & Ichiki, R. (n.d.). *Measurement of OH Radicials in Aqueous Solution Produced by Atmoshperic-pressure LF Plasma Jet.* Oita University.

Kepley, C., & Dellinger, A. (2014). Fullerenes and Their Potential in Nanomedicine. In A. D. Kelkar, D. J. Herr, & J. G. Ryan, *Nanoscience and Nanoengineering Advances and Applications* (pp. 147-164). Taylor & Francis Group.

Kroto, H. (2015). Introduction. *C60 Buckminsterfullerene: Some Inside Stories*, 1-34.

Lachance, B., Hamzeh, M., & Sunahara, G. I. (2013). Environmental Fat and Ecotoxicology of Nanomaterials. In I. Malsch, & C. Emond, *Nanotechnology and Human Health* (pp. 177-210). Taylor & Francis Group.

Lee, C. H., Linb, H. P., Line, T. S., & Mou, C. Y. (2003). Free Radical Attack on C60 Embedded in Nanochannels of Mesoporous Silica. In Z. Tang, & P. Sheng, *Nano Science and Technology Novel Structures and Phenomena* (pp. 142-147). Taylor & Francis Gropu.

Levi, N., Hantgan, R. R., Lively, M. O., Carroll, D. L., & Prasad, G. L. (2006). C60-Fullerenes: detection of intracellular photoluminescence and lack of cytotoxic effects. *Nanobiotechnology*, 1-11.

Ling, Z., & Yanke, C. (2016). *Nano-coax of C60: Molecular Cabling for Photovoltaics*. Retrieved 2016, from http://www.tvc.utah.edu/techpublisher/energy_environment/4646.php

Lipid Peroxidation. (n.d.). Retrieved 2016, from http://www.cellbiolabs.com/lipid-peroxidation

Lloyd, W. R., Chen, L.-C., & Mycek, M.-A. (2014). Fluorescence. In S. P. Morgan, F. R. Rose, & S. J. Matcher, *Optical Techniques in Regerative Medicine* (pp. 171-203). Taylor & Francis Group.

Mackay, C. E., & Hamblen, J. (2008). Toxicology and Risk Assessment. In K. Sellers, C. Mackay, L. L. Bergeson, S. R. Clough, M. Hoyt, J. Chen, . . . J. Hamblen, *Nanotechnology and the Environment* (pp. 193-224). Taylor & Francis Group.

Masschelein, W. J. (2002). Use of Ultraviolet in Photochemical Synergistic Oxidation Processes in Water Sanitation. In W. J. Masschelein, & R. G. Rice (Ed.), *Ultraviolet Light in Water and Wastewater Sanitation* (pp. 4-1-4-21). Lewis Publishers.

Mondal, S., & Purkayastha, P. (2016). Hollow Fluorescent Carbon Nanoparticles. In K. D. Sattler, *Carbon Nanomaterials Sourcebook: Nanoparticles, Nanocapsules, Nanofibers, Nanoporous Structures, and Nanocomposites* (pp. 353-362).

Mroz, P., Huang, Y.-Y., Wharton, T., & Hamblin, M. R. (2010). Fullerenes in Photodynamic Therapy of Cancer. In K. D. Sattler, *Handbook of Nanophysics: Nanomedicine and Nanorobotics* (pp. 37-1-37-20). Taylor & Francis Group.

Nadeau, J. (2013). Quantum Dot Reactive Oxygen Species Generation and Toxicity in Bacteria: Mechanisms and Experimental Pitfalls. In J. F. Callan, & F. M. Raymo (Eds.), *Quantum Dot Sensors: Technology and Commercial Applications* (pp. 6-1-6-41). Pan Stanford Publishing Pte. Ltd.

Nalabotu, S. K., & Blough, E. R. (2013). Toxicology of Nanoparticles. In A. Kumar, H. M. Mansour, A. Friedman, & E. R. Blough (Eds.), *Nanomedicine in Drug Delivery.*

Nalabotu, S. K., & Blough, E. R. (n.d.). Toxicology of Nanoparticles. In A. Kumar, H. M. Mansour, A. Friedman, & E. R. Blough (Eds.), *Nanomedicine in Drug Delivery.*

Nipun. (2015). *Difference Between Absorbance and Transmittance*. Retrieved 2016, from http://pediaa.com/difference-between-absorbance-and-transmittance/

O'Brien, S. C. (2015). The discovery of the fullerenes. *C60 Buckminsterfullerene: Some Inside Stories* , 1-13.

Ohkubo, K., Kohno, N., Yamadaa, Y., & Fukuzumi, S. (2015). Singlet oxygen generation from Li C60 nano-aggregates dispersed by laser irradiation in aqueous solution. *ChemComm* , 8082-8085.

Oram, B. (n.d.). *Ozonation in Water Treatment*. Retrieved 2016, from http://www.water-research.net/index.php/ozonation

Osawa, E. (2015). How I conceived soccerball molecule C60 . *C60 Buckminsterfullerene: Some Inside Stories* , 1-9.

Poljak-Blazi, M., Jaganjac, M., & Zarkovic, N. (2010). Cell Oxidative Stress: Risk of Metal Nanoparticles. In K. D. Sattler, *Handbook of Nanophysics: Nanomedicine and Nanorobotics* (pp. 16-2-16-17). Taylor & Francis.

Quanjun, X., Jiaguo, Y., & Po, W. K. (2011). Journal of Colloid and Interface Science. *Quantitative characterization of hydroxyl radicals produced by various photocatalysts*, 163-167.

Rahmani, A., & Chadli, H. (2010). Structure and Vibrations in C60 Carbon Peapods. In K. D. Sattler (Ed.), *Handbook of Nanophysics: Clusters and Fullerenes* (pp. 46-1-46-29). Taylor & Francis Group.

Reckhow, D. (n.d.). *Natural Organic Matter in Water*. Retrieved 2016, from http://www.ecs.umass.edu/eve/research/STEM/NOM%20and%20treatment%20abb%20v3.pdf

RF-6000 Spectrofluorophotometer. (2016). Retrieved 2016, from http://www.shimadzu.com/an/molecular_spectro/fluoresence/rf6000/index.html

S, A., FG, P., & TD, P. (2012). *Methane dynamics in the Willamette River, Oregon, U.S.A.* Retrieved 2016, from http://www.stccmop.org/publications/methane_dynamics_willamette_river_oregon_usa

Sartor, M. (n.d.). *Dynamic Light Scattering.* University of California, San Diego.

Savage, L. (2013). Artificial Photosynthesis: Saving Solar Energy for a Rainy Day. 12.

Savage, L. (2013, February). *Artificial Photosynthesis: Saving Solar Energy for a Rainy Day*. Retrieved 2016, from http://www.osa-opn.org/home/articles/volume_24/february_2013/features/artificial_photosynthesis_saving_solar_energy_for/

Sayesa, C. M., Gobinb, A. M., Ausmanc, K. D., Mendeza, J., Westb, J. L., & Colvin, V. L. (2005). Nano-C60 cytotoxicity is due to lipid peroxidation. *Biomaterials*.

Scott, L. T. (2015). The first stepwise chemical synthesis of C60. *C60 Buckminsterfullerene: Some Inside Stories* , 1-11.

Sharma, P., Jha, A. B., Dubey, R. S., & Pessarakli, M. (2014). Reactive Oxygen Species Generation, Hazards, and Defense Mechanisms in Plants under Environmental (Abiotic and Biotic) Stress Conditions. In M. Pessarakli (Ed.), *Handbook of Plant and Crop Physiology* (pp. 509-548). Taylor & Francis Group.

Shimadzu Corporation. (1875). *RF - 5301 PC.* Retrieved from Shimadzu Spectrofluorophotometer: http://www.ssi.shimadzu.com/products/literature/Spectroscopy/C125-E008F.pdf

Siggel, U., & Fuhrhop, G. L.-H. (2004). Photochemistry of Membrane-Coated Nanoparticles. In S. E. Lyshevski, *Dekker Encyclopedia of Nanoscience and Nanotechnology.* Marcel Dekker, Inc.

Sincero, A. P., & Sincero, G. (2002). Coagulation. In A. P. Sincero, & S. G. A., *Physical-Chemical Treatment of Water and Wastewater* (pp. 12-1-12-48). Taylor & Francis.

So, P. T., & Dong, C. Y. (2012). Fluorescence Spectrophotometry. *Encyclopedia of Life Sciences*, 4.

Spellman, F. R. (2003). Water Treatment Operations and Unit Processes. In *Handbook of Water and Wastewater Treatment Plant Operations* (pp. 17-1-17-65). Lewis.

Spellman, F. R. (2003). Water Treatment Operations and Unit Processes . In F. R. Spellman, *Handbook of Water and Wastewater Treatment Plant Operations* (pp. 17-1-17-65). Lewis Publishers.

Stump, K. L. (2009). *Examination of nana-C60 aggregates through dialysis membranes as surrogates for cell membrane diffusion.* Washington State University.

Tang, W. Z. (2003). Ultraviolet/Hydrogen Peroxide. In W. Z. Tang, *Physicochemical Treatment of Hazardous Wastes* (pp. 229-283). Lewis Publishers.

The Transmission Electron Microscope. (2016). Retrieved 2016, from http://www.nobelprize.org/educational/physics/microscopes/tem/

Tratnyek, P. G., & Macalady, D. L. (2000). Oxidation-Reduction Reactions in the Aquatic Environment . In R. S. Boethling (Ed.), *Handbook of Property Estimation Methods for Chemicals: Environmental and Health Sciences* (pp. 16-1-16-35). Taylor & Francis Group.

Unwin, P. (1990). *Fullerenes: An Overview*. Retrieved from http://www.ch.ic.ac.uk/local/projects/unwin/

Usenko, C. Y., Harper, S. L., Simonich, M. T., & Tanguay, R. L. (n.d.). Fullerene C60 Toxicology . In K. D. Sattler, *Handbook of Nanophysics: Nanomedicine and Nanorobotics* (pp. 17-1-17-8). Taylor & Francis Group.

UV Light Systems Information. (2016). Retrieved 2016, from http://www.globalspec.com/learnmore/optics_optical_components/light_sources/process_uv_lamps_systems

Valsaraj, K. T. (2000). Applications of Chemical Kinetics in Environmental Systems. In K. T. Valsaraj, *Elements of Environmental Engineering: Thermodynamics and Kinetics* (pp. 267-423). Taylor & Francis.

Ventra, M. D., Evoy, S., & Heflin, J. R. (2004). *Introduction to Nanoscale Science and Technology.* (M. D. Ventra, S. Evoy, & J. R. Heflin, Eds.) New York, New York, USA: Springer Science + Business Media Inc.

Vidal, L., Domini, C. E., & Canals, A. (n.d.). Main Parameters and Assays Involved with the Organic Pollution of Water. In L. M. Nollet, & L. S. Gelder, *Handbook of Water Analysis* (pp. 17-1-17-5). Taylor & Francis Group.

Wharton, L. (2015). History of "the nozzle". *C60 Buckminsterfullerene: Some Inside Stories* , 1-7.

Wray, L. (2001-2008). *Leading the development of nanostructured carbon products*. Retrieved 2016, from file:///Volumes/ILY_KELSEY/MQP%20things/Nano-C%20%20Fullerenes%20%20Applications.html

Yu, Q.-W., & Feng, Y.-Q. (2010). HPLC Separation of Fullerenes. In K. D. Sattler, *Handbook of Nanophysics: Clusters and Fullerenes* (pp. 22-1-22-5). Taylor & Francis.

Zhao, H., Wang, L., Zhang, Z., Zhao, B., Yao, Y., & Zhang, H. (2014). Preoxidation with potassium permanganate in the coagulation- ultrafiltration process for micro-polluted water treatment. *Environment, Energy and Sustainable Development* , 461-465.

Zheng, L., Chen, W., Li, J., & Yue, S. (2016). Advanced treatment of rainwater by H2O2/UV process. In Kim, *Progress in Civil, Architectural and Hydraulic Engineering IV* (pp. 1371-1375). London: Taylor & Francis Group.

Zoro, I. (2011-2016). *Zoro Products*. Retrieved from Zoro: https://www.zoro.com/johnson-controls-install-kit-std-26in-pvc-pipe-f-std-instl13/i/G0944590/

Appendix

A: Spectrophotometry

All other examinations and the corresponding data to each fluorescence spectra measured.

Table A 1: Varied pBS Volume

Vials	TA (10 mM)	H_2O_2 (30%)	nC_{60}	pBS (10 mM)	Final Concentration
1	4 mL	4 mL		32 mL	8 mM
2	4 mL	4 mL	13 mL	19 mL	4.75 mM
3	4 mL	4 mL	26 mL	6 mL	1.5 mM
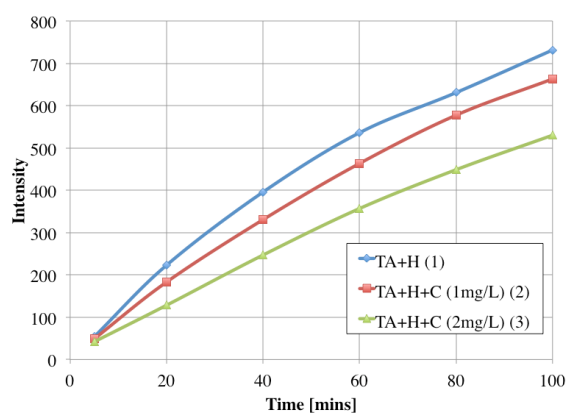
Figure A 1: Varied pBS Volume Intensity

Table A 2: Lower TA Value

Vials	NaOH (100 mM) TA (20 mM)	H_2O_2 (30 mg/L)	nC_{60} (9.88 mg/L)	H_2O	pH
1	2 mL	4 mL		34 mL	11.41
2	2 mL	4 mL	4 mL	30 mL	11.42
3	2 mL	4 mL	16 mL	18 mL	11.40
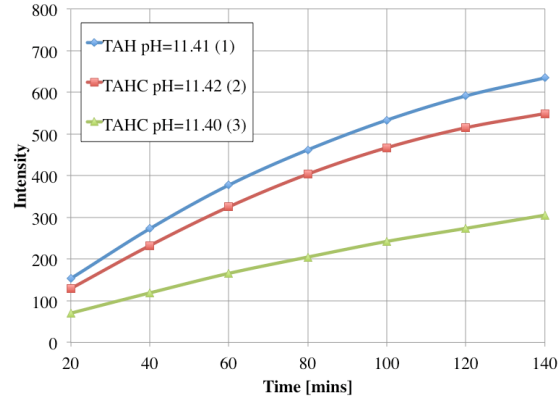
Figure A 2: Lower TA Value

Table A 3: Higher nC60 Value

Vials	NaOH (100 mM) TA (20 mM)	H_2O_2 (30 mg/L)	nC_{60} (9.88 mg/L)	H_2O	pH
1	2 mL	4 mL		34 mL	11.46
2	2 mL	4 mL	8 mL	26 mL	11.52
3	2 mL	4 mL	32 mL	2 mL	11.48
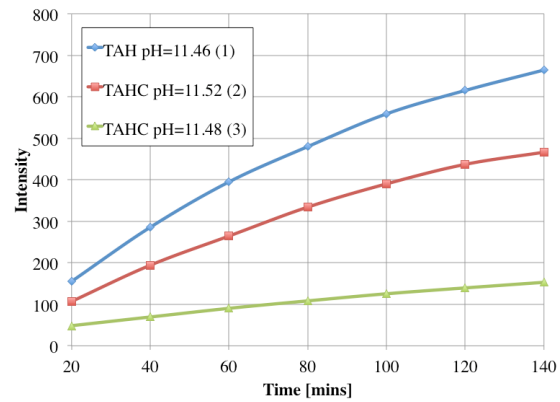
Figure A 3: Higher nC60 Value

Table A 4: Water Added for Dilution

Vials	NaOH (200 mM) TA (20 mM)	H_2O_2 (30 mg/L)	nC_{60} (9.88 mg/L)	H_2O	pH
1	2 mL	4 mL		34 mL	12.04
2	2 mL	4 mL	4 mL	30 mL	12.05
3	2 mL	4 mL	16 mL	18 mL	12.09
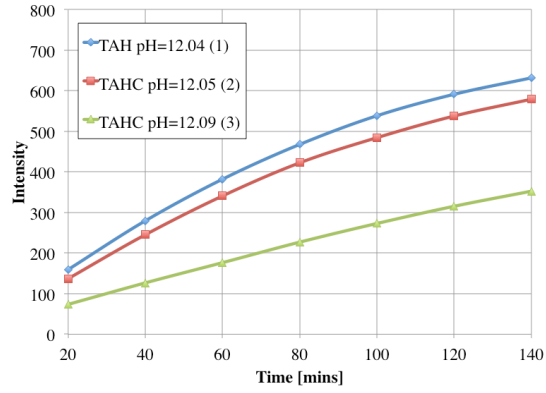
Figure A 4: Water Added for Dilution

Table A 5: Variable Changes

Vials	TA (10 mM)	H$_2$O$_2$ (30%)	nC$_{60}$	pBS (200 mM)	Final Concentration	HCl (1M)	pH
1	4 mL	4 mL		31.5 mL	9 mM	0.5 mL	9
2		4 mL		36 mL	9 mM	0.5 mL	5.5-6
3	4 mL		13 mL	23 mL	5.75 mM	0.5 mL	9
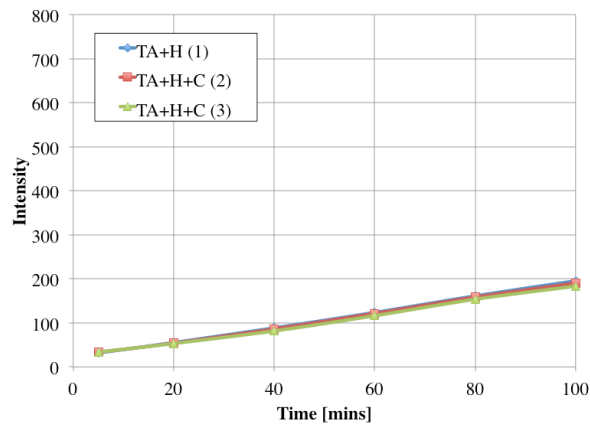
Figure A 5: Variable Changes

B: High Performance Liquid Chromatography
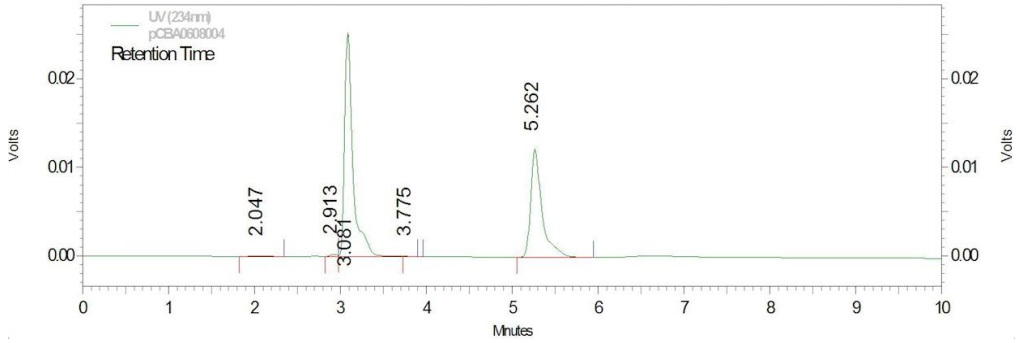
Figure B 1: Chromatogram Image from the HPLC analysis

Table B 1: Raw Data for Trial 1 using HPLC

Time (min)	Sample #		1	2	3
	1	Rt	5.427	5.429	5.417
		A	64878	193481	182180
		H	6961	19867	19785
5	2	Rt	5.425	5.420	5.428
		A	166544	46977	15671
		H	18169	4938	21270
	3	Rt	5.442	5.419	5.422
		A	60016	185153	198815
		H	6329	20196	21654
	1	Rt	5.424	5.416	5.420
		A	198202	193788	173739
		H	21459	21005	19055
20	2	Rt	5.422	5.423	5.416
		A	198573	192552	193801
		H	21746	20908	20973
	3	Rt	5.421	5.418	5.425
		A	200037	194568	193767
		H	21854	21289	20978
	1	Rt	5.419	5.472	5.449
		A	193506	188724	179037
		H	21091	20476	18816
40	2	Rt	5.428	5.466	5.457
		A	196250	193007	181977
		H	21334	20956	19727
	3	Rt	5.444	5.481	50441
		A	194196	193991	153622
		H	21021	21075	16617
	1	Rt	5.443	5.450	5.453
		A	162793	177896	174070
		H	17768	18865	18816
60	2	Rt	5.460	5.447	5.460
		A	199354	189351	184219
		H	21378	20272	20005
	3	Rt	5.457	5.466	5.460
		A	177435	163541	171876
		H	19161	17670	18750
	1	Rt	5.454	5.419	5.442
		A	205994	156092	181504
		H	22178	17076	19701
80	2	Rt	5.462	5.427	5.420
		A	164215	143569	165052
		H	17677	15642	17767
	3	Rt	5.451	5.419	5.490
		A	19698	176884	189362
		H	21021	19252	20363
	1	Rt	5.480	5.475	5.476
		A	193223	186280	165237
		H	20620	19920	17691
100	2	Rt	5.474	5.472	5.462
		A	188033	165566	188027
		H	19153	17823	20004
	3	Rt	5.477	5.486	5.477
		A	201198	185470	186011
		H	21533	19855	20024

Vials	pCBA (30 mg/L)	H_2O_2 (1.5 g/L)	nC_{60}	H_2O	pH
1	4 mL	4 mL		32 mL	10.18
2	4 mL	4 mL	13 mL	19 mL	9.68
3	4 mL	4 mL	26 mL	6 mL	9.44

Table B 3: HPLC Data Trial 2

Time (min)	Sample #		1	2	3
	1	Rt	5.398	5.391	5.392
		A	199959	193684	187092
		H	21042	19932	19302
5	2	Rt	5.375	5.391	5.397
		A	193972	197845	197301
		H	20015	20241	20432
	3	Rt	5.376	5.400	5.400
		A	195188	198857	185333
		H	20127	20623	19162
	1	Rt	5.403	5.437	5.452
		A	190687	88724	194334
		H	20104	20016	20506
20	2	Rt	5.417	5.430	5.483
		A	193228	166126	188366
		H	20256	17308	16511
	3	Rt	5.433	5.442	5.460
		A	194230	178468	182246
		H	20543	18681	18880
	1	Rt	5.485	5.460	5.470
		A	244576	182208	190530
		H	19133	18822	19485
40	2	Rt	5.498	5.465	5.468
		A	234670	188633	187549
		H	19689	19225	19564
	3	Rt	5.476	5.470	5.461
		A	237488	183718	181159
		H	20538	18978	18942
	1	Rt	5.459	5.446	5.439
		A	171674	176560	1639670
		H	17870	18360	17574
60	2	Rt	5.463	5.434	5.437
		A	170153	192806	142113
		H	17969	20106	14812
	3	Rt	5.433	5.440	5.433
		A	109634	157850	164044
		H	11393	16224	16739
	1	Rt	5.416	5.434	5.432
		A	179407	157839	173622
		H	18702	16412	18079
80	2	Rt	5.434	5.436	5.422
		A	187147	153043	166857
		H	19619	15864	17398
	3	Rt	5.416	5.418	5.428
		A	179407	187772	129847
		H	18702	19358	13286
	1	Rt	5.434	5.425	5.439
		A	187147	158664	196386
		H	19619	16160	20458
100	2	Rt	5.430	5.432	5.446
		A	197616	71462	150217
		H	20694	18000	15473
	3	Rt	5.430	5.439	5.440
		A	186222	151065	165153
		H	19532	15572	17322